Ana Luísa Vicente Ruivo Nunes

Colheita de energia para aplicações IoT em ferrovia

Energy harvesting for railway IoT applications

Universidade de Aveiro
2022

Ana Luísa Vicente Ruivo Nunes

Colheita de energia para aplicações IoT em ferrovia

Energy harvesting for railway IoT applications

Dissertação apresentada à Universidade de Aveiro para cumprimento dos requisitos necessários à obtenção do grau de Mestre em Engenharia Eletrónica e Telecomunicações, realizada sob a orientação científica do Doutor Nuno Borges de Carvalho, Professor catedrático do Departamento de Eletrónica, Telecomunicações e Informática da Universidade de Aveiro.

o júri / the jury

presidente / president

Professor Doutor Telmo Reis Cunha

Professor Associado no Departamento de Eletrónica, Telecomunicações e Informática da Universidade de Aveiro

vogais / examiners committee

Professor Doutor Rodolfo Alexandre Duarte Oliveira

Professor Associado Com Agregação da Universidade Nova de Lisboa - Faculdade de Ciências e Tecnologia (arguente)

Professor Doutor Nuno Borges de Carvalho

Professor Catedrático no Departamento de Eletrónica, Telecomunicações e Informática da Universidade de Aveiro (orientador)

agradecimentos / acknowledgements

Em primeiro lugar, quero agradecer aos meus pais, à minha tia e ao meu irmão por todo o apoio prestado durante os últimos 5 anos e por tornarem tudo isto possível.

Quero agradecer também aos meus amigos, companheiros de todas as horas, por fazerem com que este percurso fosse mais fácil.

Devo ainda um especial agradecimento ao meu orientador, Prof. Dr. Nuno Borges de Carvalho, por me ter oferecido a possibilidade de elaborar esta tese, por me ter motivado e se mostrado sempre disponível para me ajudar.

Devo um agradecimento, ainda, à Prof. Dra. Paula Vilarinho, ao Rui Pinho e à Inês Loureiro, do Departamento de Engenharia de Materiais e Cerâmica da Universidade de Aveiro, pela ajuda prestada e pelos materiais cedidos no decorrer deste trabalho.

E, por último mas não menos importante, quero agradecer aos membros do Instituto de Telecomunicações e colegas do laboratório de Rádio Frequência por me terem auxiliado sempre que precisei.

Palavras Chave

recolha de energia de vibrações, ferrovia, baixa potência, coletor de energia eletromagnético, retificação, sensor indutivo, coletor de energia piezoelétrica, material piezoelétrico sem chumbo.

Resumo

O tema desta dissertação advém da necessidade de encontrar alternativas às formas convencionais de alimentar dispositivos: baterias. Contudo, este é um assunto mais importante do que possa parecer, já que a falta de energia e os custos a si associados não afetam apenas quem planeia simples redes de sensores para aplicar em ferrovia, mas sim a todos sem excepção. Portanto, este trabalho foca-se na produção de energia proveniente da vibração presente em nosso redor. Dois coletores de energia foram considerados ao longo deste trabalho: eletromagnético e piezoelétrico. Ao longo do estudo sobre o coletor eletromagnético, três protótipos constituídos por uma bobina e um íman em movimento no seu interior foram construídos. Num teste que envolveu corrida, foi atingida uma potência máxima de 9 mW com uma bobina de 170 enrolamentos, 20 cm de comprimento e 2 cm de diâmetro. Observou-se que a tensão do sinal de saída obtido era muito baixa, o que faz com que a retificação de um sinal com estas características seja um desafio. Para contornar este problema, dois circuitos de retificação foram considerados: retificador em ponte e retificador duplicador. O retificador duplicador permitiu atingir uma tensão mais alta após retificação, 23 mV, para um sinal de entrada com picos na ordem dos 160 mV. Dado isto, a potência produzida pelos protótipos não foi satisfatória, sendo óbvio que nenhum deles poderá trabalhar como coletor de energia. No entanto, estes coletores são capazes de funcionar como sensor indutivo sem necessitar de bateria. O segundo coletor de energia considerado foi um transdutor piezoelétrico, composto por material PZT (contem chumbo) e KNN (sem chumbo). Uma caracterização em função da frequência foi feita, o que permitiu uma posterior comparação entre estes dispositivos com base nas suas propriedades piezoelétricas. É claro que PZT é mais eficiente do que KNN, no entanto o material KNN apresenta propriedades piezoelétricas muito inferiores, discrepância que não se reflete na mesma dimensão na potência produzida pelos mesmos. A máxima potência obtida para um PZT foi 54 nW à frequência de 500 Hz e para um KNN foi 4.5 nW para uma frequência de 200 Hz.

Keywords

vibration energy harvesting, railway, low-power, electromagnetical harvester, rectification, inductive sensor, piezoelectric harvester, lead-free piezoelectric material.

Abstract

The subject of this dissertation comes from the urgent need of finding alternatives to the conventional way of powering devices: batteries. However, this issue is more significant than it may appear, because the lack of energy and its costs not only affect who plans a simple sensor network for a railway application, but also the entire human population. Therefore, this work focus on how to create energy from vibration that is present all around us. There were two types of harvesters considered: electromagnetic and piezoelectric. Within the electromagnetic harvester, there were three different harvesters built (coil with a moving magnet inside). During a running test, the maximum power achieved was 9 mW, with a coil of 170 turns, 20 cm long with a 2 cm diameter. It was possible to observe that the voltage produced was very low, which made rectification of a signal with these characteristics a challenge. In order to solve this problem two rectifier circuits were considered: bridge and doubler rectifier. The doubler rectifier allowed to achieve the most voltage, an average output voltage of 23 mV for an input signal with peaks of $160\ mV$. Given that the power produced by the prototypes built were not satisfactory, it is clear that none of them could function as an harvester. However, these harvesters could work properly as a battery-free inductive sensor. The second harvester considered were piezoelectrics. A characterization along frequency of PZT (lead based) and KNN (lead-free) piezoelectric materials was performed. A comparison based on their piezoelectric properties was made, it is clear that PZT piezoelectrics are more efficient than KNN ones, but KNN power production is still promising despite the fact that they have inferior properties. The maximum power achieved for a PZT piezoelectric was 54 nW for a frequency of $500\ Hz$ and for a KNN a power around $4.5\ nW$ was obtained at a frequency of 200 Hz.

Contents

List of Figures

List of Tables

Acronyms

AC Alternating Current. 11, 24

ADC Analog to Digital Converter. 20, 21

DC Direct Current. 12, 13, 24, 26, 45

IoT Internet of Things. 2, 14, 29, 42

KNN Potassium-sodium niobate. 29–31, 41–43, 46

LEDs Light-Emitting Diodes. 9

PV Photovoltaic. 9

PZT Lead zirconate titanate. 29–31, 34, 41–43, 46

RF Radio Frequency. iii, 12, 13

Rohs Restriction of Hazardous Substances Directive. 29

VISA Virtual Instrument Software Architecture. 32

WSN Wireless Sensor Networks. 2, 10, 13, 14

Chapter 1

Introduction

This document, denoted as "Energy harvesting for railway IoT applications", presents the accomplished work during the dissertation concerning the master in Electronics and Telecommunications Engineering in the department of Electronics, Telecommunications and Informatics of University of Aveiro.

This work aims to take a step further towards energy harvesting, in this case converting vibration and movement into electricity for small autonomous devices making them self-sufficient.

In this chapter, it is explained the motivation associated to this work, the proposed objectives and there is also a brief description of its structure.

1.1 Motivation

Over the past few years, public transportation has gained more importance. More and more people use train as their mean of transport everyday due to its high speed, efficiency, comfort, low cost, and the fact that is better for the environment. In Portugal, for example, in this year more than 32 millions of passengers used the train from January to March, an increment of 104% when comparing to the same period of 2021 [1]. However, with the increased numbers of passengers that look for this service, the service has also to adapt to the new reality. More people need more trains and more schedules available, as a consequence the deterioration of the infrastructure also increases. Its maintenance is a challenge because it is costly and takes a lot of time causing delays or even a reduction in the number of trains working daily. Therefore, it is crucial that problems are detected as soon as possible to provide the fastest possible troubleshooting so it has no impact on the service or on the costumers. If inspection could be made in real-time and not just only periodically by a person it would be much more efficient, faults could be detected and solved way faster. Real-time maintenance through a sensors network could be a solution. Sensors could

be placed in every carriage of every train and communicate in real-time with its train driver or technicians. Although this appears to be simple, it hides a tremendous logistical and economic challenge: batteries.

Batteries have been a constraint of every system and application, and not only railways related. More and more devices are being used in Internet of Things (IoT) and in different Wireless Sensor Networks (WSN). By 2025, the total number of installed IoT devices is expected to reach 75.44 billion globally, a fivefold growth in ten years [2]. As we know, batteries' management requires the installation, maintenance and further replacement after their durability has run out. It will be impractical in the future to handle perhaps millions or even billions of devices individually, not to mention expensive due to the maintenance cost. The bottom line is that batteries will have no role in most technology in the foreseeable future. So, this is one strong reason why the demand for alternative energy sources is rapidly increasing.

Another reason is that we are living an energy crisis. Energy problems affect every individual, company, institution and country. Therefore, energy has become an emerging topic, there is always a politician or a world association discussing this subject daily. Although the costs related to energy are not a recent concern, since the beginning of the war in Ukraine many experts have been foreseeing how much more this is going to prejudice us all. Russia's natural gas exports to Europe have considerably decreased since the West adopted strict sanctions and as a consequence the prices have gone up. This can be seen in figure 1.1 where the gray vertical stripe marks when the war started. Every government of every country is now trying to solve this problem by eliminating their dependency on Russia's gas. As an example, European countries are looking for green solutions and European Union was already pointed a possible one: Portugal and Spain, which are expected to turn Europe self-sufficient in terms of energy because of the wealth of renewable resources in the Iberian Peninsula.

From an environmental perspective, until now, the bulk of the world's power needs have been met by exploitation of non-renewable fossil fuels, which are known to be running out. With our rapidly growing population, our energy urge will continue to expand, and worldwide energy expenditure is predicted to reach 777 quintillion Joules by 2040 while now it is already at 607 quintillion joules each year [4]. This growth in consumption can be seen in figure 1.2 that refers to the last century. As a result of this tremendous increase, the pursuit of a renewable energy source that can meet our ever-increasing demands has become an urgent topic. Hence, energy harvesting holds a lot of promise.

Energy harvesting is as simple as absorbing and transforming energy from the environment into electricity. There are various sources: light, thermal, vibration, nuclear, biomass, hydropower, wind and acoustic energy present in the surroundings of a device. When energy harvesting is used it

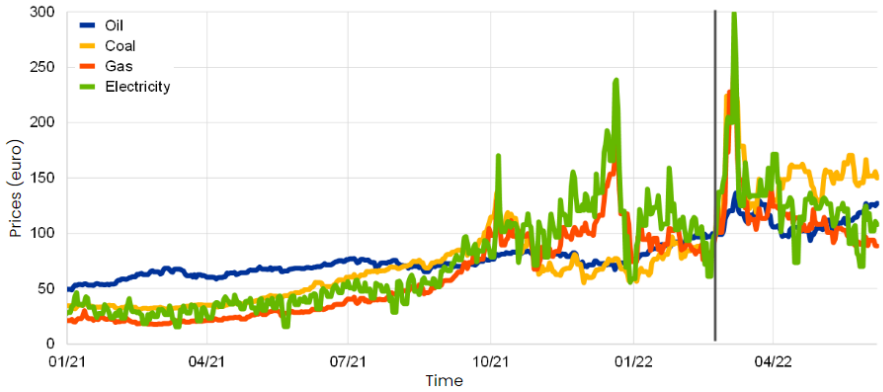

Figure 1.1: Energy prices before and after the invasion of Ukraine. (Retrieved from [3])

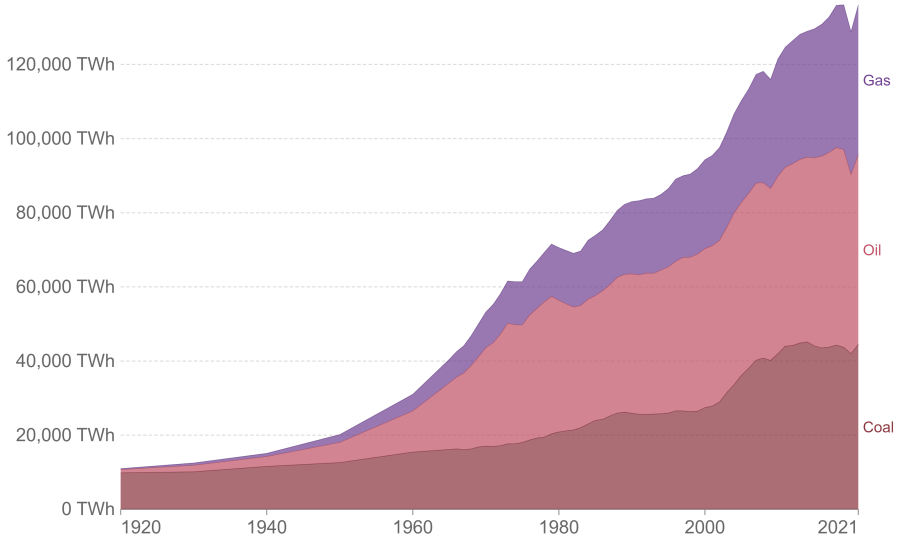

Figure 1.2: Global fossil fuel consumption from 1920 to 2021. (Retrieved from [5])

---

provides a mean of powering a device without the need for a conventional power source, therefore there is no need to use wires or even to replace a battery, which leads to a minimization of maintenance costs and turns these devices into ecological solutions. These kinds of harvesters are also useful for applications in which the use of conventional batteries are not suitable such as underwater or out of reach places.

Numerous energy harvesting alternatives have been found, studied and even applied to low-power applications. Although the harvested energy is usually small and in the order of milliwatts, it can provide enough power for

wireless sensors and other low-power applications. It isn't the fix to all of our energy concerns, but it does make a promise when it comes to delivering electricity to low-power devices.

1.2 Objectives

This work focuses on different ways of harvesting energy on a train, considering one source: kinetic energy which is a consequence of its movement or vibration.In order to understand how we can get the most efficiency out of it, different harvesters and approaches within the same harvester will be studied and their performance compared. To achieve what was stated above the goals along this dissertation are:

- Theoretical study on electromagnetic induction as an energy harvesting source;
- Implementation and comparison of various prototypes of the electromagnetic vibration harvester;
- Understand how different parameters, as length, wire width, windings, frequency, so on, of the harvester influence its power generation;
- Theoretical study on piezoelectricity as an energy harvesting source;
- Understand how frequency influences piezoelectrics power generation;
- Comparison of the piezoelectrics based on the input frequency and the material they are made of;

1.3 Document Organization

This document is organized as follows:

- Chapter 1 contextualizes and describes the importance of this dissertation's theme and also its goals;
- Chapter 2 gives an overview of energy harvesting, presenting concepts related to this subject, different energy sources, types of harvesting and transducers as well as various example of what have been done in this field regarding each source;
- Chapter 3 presents the work principle of an electromagnetic harvester, a theoretical analysis, how each prototype was built and their characteristics, the experiments made and the results obtained related to all devices;

- Chapter 4 describes the work principle of piezoelectricity and presents a study on the influence of the frequency of six different samples that differ on size and material, and also a comparison between them based on the power generated and piezoelectric properties;
- Chapter 5 concludes the developed work and proposes possible future work to improve the performance of the harvesters.

Chapter 2

State of Art

Based on the existing literature and research, this chapter gives an outline of energy harvesting and the various approaches within this subject. There is also a overview on different harvesters and their working principle as well as what has already been done with respect to the various energy sources.

2.1 Energy harvesting

Energy harvesting, also known as energy scavenging or ambient power, is a method in which energy is scavenged and converted from sources such as mechanical load, vibrations, temperature gradients, light, among others, that otherwise would be dissipated or wasted. [4] The energy can either be used immediately or stored for future use. Energy harvesting can only obtain power in the nW-mW range, but it can be enough in certain applications.

Although this appears to be the best way to make small sensors wireless and self-contained while also eliminating the need for maintenance, there are significant drawbacks. Because it is dependent on external factors, energy harvesting power is likely to be weak and unstable. Unexpected shutdowns must also be taken into account. As a result, more advanced energy harvesting technologies will continue to grow and evolve in the future.

Another limitation is that most vibration-based harvesters have a narrow bandwidth. These devices will only produce maximum power when the generator's resonant frequency meets the frequency of the ambient vibration. Any difference in frequency between these two can result in a substantial decrease in generated power which is very probable given that mechanical and human motion vibrations have a wide frequency spectrum. Various strategies have been offered for enhancing the operating bandwidth of linear harvesters. However, most of these methods have downsides, such as increased complexity, less power generation, the need for additional systems and energy, low efficiency, difficulties in implementation, and so on. [6]

2.2 Energy harvesters

Depending on the type of energy source, there are many different types of energy collecting devices. Nevertheless, on their most basic form all energy harvesting systems include three primary components in addition to a source of energy:

- The harvester, which is nothing more than a simple transducer, converting ambient energy from the source into electrical energy.
- The interface circuit, which collects the maximum quantity of energy from the transducer and converts it into a usable form for the chosen application through voltage regulation, rectification or similar.
- The load, which depending on the goal can be the part that will use the energy collected or just store it. Therefore, the load can be many things, on one hand sensors, actuators, circuits and on the other hand energy storage components as a capacitor, a battery or even a power management unit.

An illustration of the main components of an energy harvesting system as well as examples of different energy sources are shown in figure 2.1.

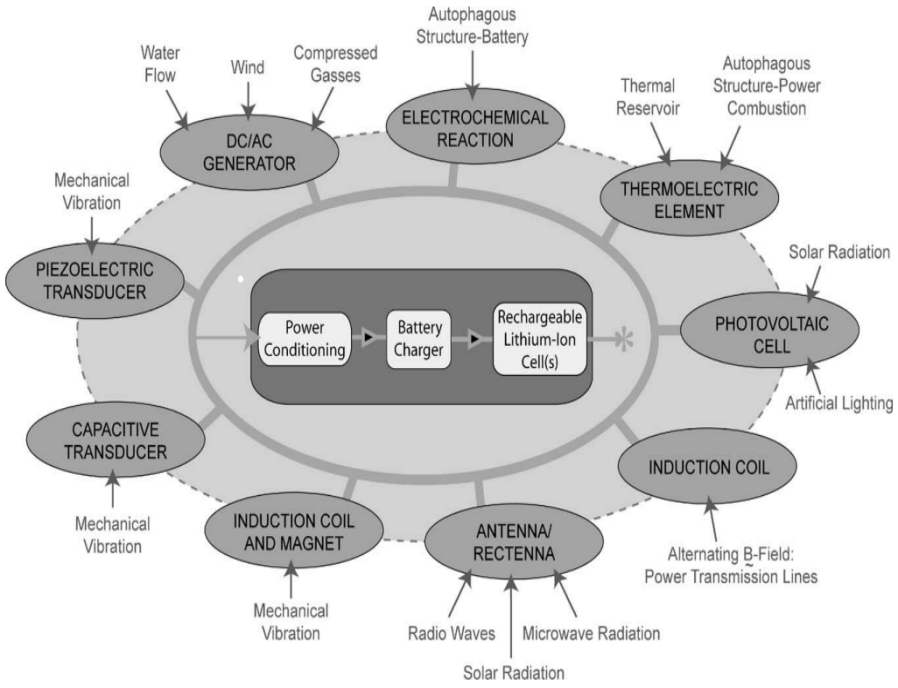

Figure 2.1: Different energies sources that can be converted into electrical energy. (Retrieved from [7])

2.2.1 Solar energy harvesting

Solar energy harvesting is one of the most common types of harvesting. It can be already found installed inside a house, school, company, among others, or outside where it is the most efficient. Photovoltaic cells are used to gather solar energy and by means of the "photovoltaic effect" they transform solar energy directly into electricity. The photovoltaic effect is the process by which photons (units of light energy) stimulate electrons into a higher energy state, resulting in the generation of an electric current. This is illustrated in figure 2.2.

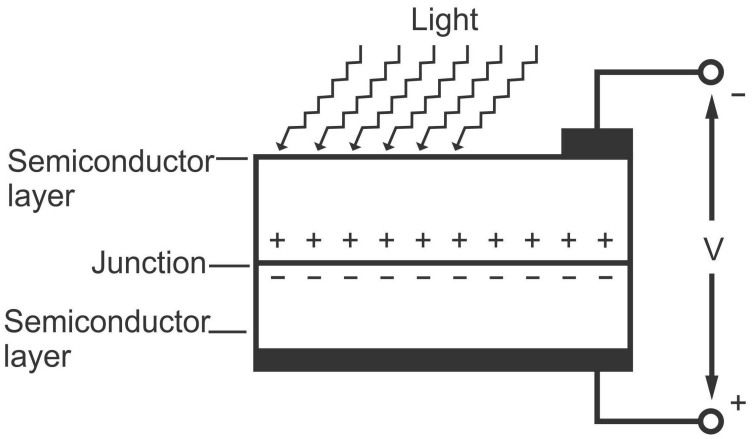

Figure 2.2: Schematic of photovoltaic effect. (Retrieved from [8])

Photovoltaic (PV) cells are classified into four types: single and multi-junction cells, thin-film cells, crystalline Si cells and emerging technologies. PV cells are often pricey. Instead of PV cells, Light-Emitting Diodes (LEDs) and photodiodes can be used to harvest light energy and power low-power devices like IoT edge devices. LEDs are less costly whereas photodiodes are more expensive than LEDs but provide more energy.

Harvesting light can happen indoor or outdoor. Indoor, solar panels collect mostly artificial light which is weaker. Due to the stated fact, it is usually used to feed low-power devices, for instance a wireless sensor node [9]. The research on this topic is extensive, it has already been shown an increment of 950% of the battery life of a wearable body sensor node by using a 19 $cm \times 4$ cm flexible photovoltaic module with only 2.9 mW/cm^2 of irradiance [10]. Outdoor, the efficiency is much higher especially if the sunlight hits the photovoltaic cells with an optimum incident angle. To maximize the efficiency of this harvester a maximum power point tracking device should be used in order to bypass different factors such as the intensity of the light, the incident angle, size and type of the solar panels, etc, and of course, the fact that we do not have light all day. In 2020, solar harvesting

was thought to be applied on roads, the initial findings are promising and show that a semi-transparent layer can be used in large-scale applications in the future [11].

2.2.2 Mechanical energy harvesting

Mechanical energy exists everywhere. Household products, moving objects such as automobiles and airplanes, and structures such as buildings and bridges, as well as human motion or even noise, all have vibrations. This is why kinetic energy can be seen as an endless source of power. In addition, this kind of energy harvesting has the advantage of being clean, stable and small sized. The source of this energy can be electromagnetic vibration, electrostatic vibration, piezoelectric vibration, turbines of wind or water, among others. In some cases, a combination of various sources mentioned above can be made in order to maximize the energy harvested. [12]

This energy has been harvested in a variety of scenarios, for example: biomedical device monitoring systems, airplanes, helicopters, ships, wind generator blades, bridges, and other high-rise constructions with vibrations. For instance, it has been proved that it can provide enough power for communication devices and wireless sensors to operate. [13]

2.2.2.1 Electromagnetic vibration

Michael Faraday was the first to use electromagnetic harvesters. He used it in his electric motor in which magnetic induction was the principle the motor was based.

Electromagnetic generators make use of the relative motion between a conductor and a magnetic flux to induce charge in the conductor. These generators can be divided into three types: resonant, rotating and hybrid devices. Resonant generators operate in an oscillating mode. They mainly harvest power from environmental vibrations by using the displacements between a magnet and a coil as it is illustrated in figure 2.3. Rotational generators, on the other hand, function similarly to large-scale magnetic generators. They are made to operate on rotational power from small turbines or heat engines that can supply constant rotational motion with a constant driving torque as shown in figure 2.4. Finally, hybrid devices use an uneven rotor to turn linear action into rotational motion. [14]

The biggest benefit of this type of transducer is its ease of manufacture, which ensures its reliability. Electromagnetic energy harvesters can also be macro-scale in size, making them simple to implement. Nonetheless, the low voltage output is a big drawback.

An example of a resonant generator was achieved in Turkey where it was presented a WSN whose sensors were charged using an electromagnetic

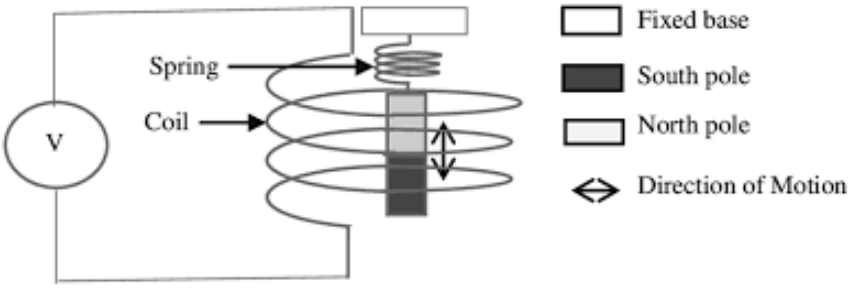

Figure 2.3: Schematic of a resonant electromagnetic generator. (Retrieved from [15])

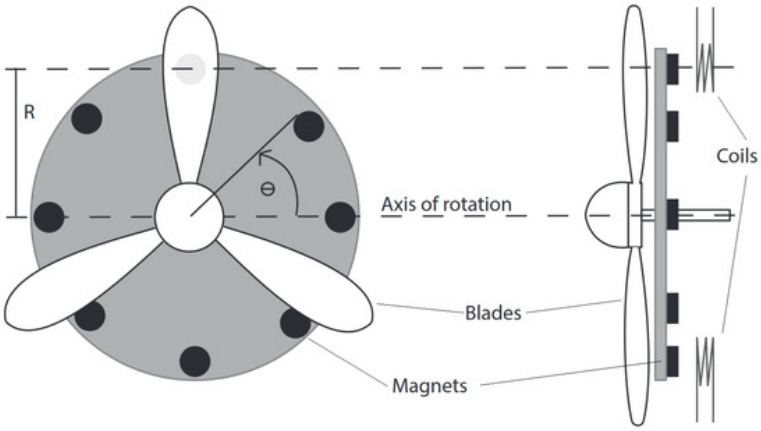

Figure 2.4: Schematic of a rotational electromagnetic generator. (Retrieved from [16])

---

vibration energy harvester. This harvester provided 65 μA charging current which was excited at $0.4g$ acceleration at 7.4 Hz. [17]

2.2.2.2 Piezoelectric vibration

Piezoelectric energy harvesters have been widely used due to their high power densities. Piezoelectricity is defined by Briscoe and Dunn [18] as the "electric charge that accumulates in response to applied mechanical stress in materials that have non-centrosymmetric crystal structures". Meaning that by exerting stress on the piezoelectric material, the vibration factor causes it to bend and generate an electric charge as illustrated in figure 2.5. The kinetic energy can be in the form of vibrations, sounds, stress or strain, then it is converted into an Alternating Current (AC) current by the transducer which will be conditioned and stored in a battery or consumed by a load.

This mechanical strain can be generated by humans which will lead to implanted and wearable electronics. [12] However, the created movement

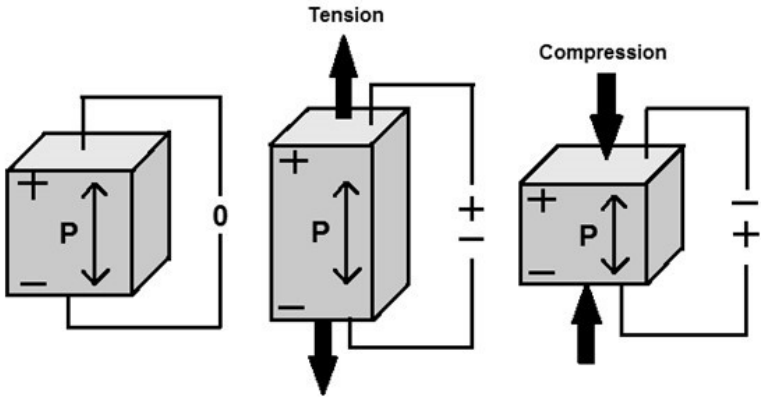

Figure 2.5: Piezoelectric behavior when mechanical stress is applied. (Retrieved from [19])

will have large amplitude at low frequencies, that is why in most applications the piezoelectric path is coupled either through direct straining or by impacting the kinetic driving source. [14] According to previous research, the greatest power created by a 68 kg person walking at a speed of 2 $steps/s$ and a heel movement of 5 cm is 67 W. [20]

Vibration-based cantilever is another method of mechanical strain creation. The most popular geometry for harvesting energy from vibrations is a piezoelectric cantilever beam. It can be unimorph, with only one piezoelectric layer on top of the beam, or bimorph, with piezoelectric layers on both surfaces of the beam. Low resonant frequencies are achieved in a low-volume construction with high levels of strain in the piezoelectric layers, which is further decreased by the addition of a mass at the end of the beam. [21]

Depending on the purpose, piezoelectric energy harvesters can be of various sizes, and they are considered simple to implement. Another big advantage is the fact that it is easily produced since it is made of small components.

2.2.3 Radio Frequency energy harvester

Radio Frequency (RF) energy can be found all around us. The environment is constantly being bombarded with radio frequency waves from a variety of sources, including, Wi-Fi, radio stations, mobile base stations, and TV towers, among others.

Because of its simplicity and ease of application, wireless energy harvesting has emerged as a RF harvesting technique. The most crucial part of this harvester is the rectifying antenna, also known as rectenna, which consists of an antenna and a rectifying circuit with a diode or CMOS. The antenna captures the signal and converts it from RF to Direct Current (DC). [22] A illustration of the components needed for a RF signal power a device can be

found in figure 2.6.

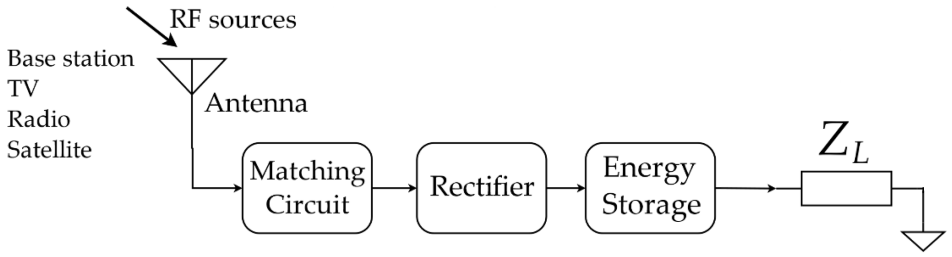

Figure 2.6: RF energy harvesting scheme. (Retrieved from [23])

There are two types of energy sources: near-field and far-field. Near-field harvesting makes use of electromagnetic induction and also magnetic resonance. These phenomena allow to produce energy that can feed a low-power device at a maximum distance of a wavelength. On the other hand, far-field harvesting can power a device within a couple kilometers because the transmitter supplies the same amount of energy constantly. However, this is not exactly true, the power received drops in respect to source distance but just not as drastically as in the near-field.

Research on RF energy harvesting has been done at the University of Washington where it was created the first battery-free phone based on RF harvesting, it only consumes 3.48 μW. [24] Also, when improvements were made in addition to the traditional RF to DC converter circuit such as adding a tuner, which consists of a capacitor and inductance in parallel, in order to select the carrier frequency and turn it into a fixed frequency value helpful for further processing. The resulting output power was measured at a distance of 77.84 m from the source, a TV tower operating at 165 MHz, having achieved a power of 1.8 mW. This made possible to power a low-power wireless device without needing a battery. [25]

Although the commercialization of this kind of harvester would be easy, it has the disadvantage that the power generated is normally around microwatts. Therefore, one big challenge in this matter is to develop a rectifying circuit to boost the efficiency of such a little radio wave input. [26]

2.2.4 Thermal energy harvester

As almost all electrical systems emit heat, a large amount of energy is being dissipated everywhere. The heat found in industrial or just high temperature environments can and should be used. For example, when deploying a WSN, the sensor nodes can be in many different places, some of which might have ambient thermal gradients that can be exploited to generate power using a thermoelectric generator.

A thermoelectric generator is a combination of thermocouples. A ther-

mocouple consists of two different kinds of metals joined together at one end. By heating one face and cooling the other, meaning a temperature difference between the two conductors or semiconductors, there will be an electrical current generated. [27] The principle of a thermocouple is shown in figure 2.7. This is known as the Seebeck effect and it was discovered in 1821 by Tomas Seebeck.

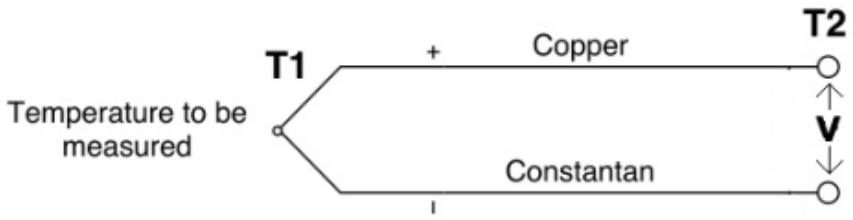

Figure 2.7: Thermocouple functioning scheme. (Retrieved from [28])

The first example of this type of harvesting is the Seiko Thermic Watch which is fully powered by a thermal harvester. A thermoelectric generator converts the body heat into electrical energy that powers the watch. It can harvest 22 W with just 1 K temperature difference between the wrist and the surroundings. [29]

A thermoelectric generator has appealing properties such as a long life cycle, no moving parts, it is also simple and reliable. However, the low efficiency of this technique has consistently hindered its commercial potential.

2.3 Summary

IoT and WSN markets are exploding, in just a few years the number of devices will turn into billions and they are going to be present everyhere. The biggest challenge is how to power them all and that is why energy harvesting is thriving. Replacing the batteries and, consequently, the cost of maintenance will no longer be a problem.

This chapter provided an overview of different energy harvesting techniques, their operation principle, their potential, advantages as well as limitations which some of them are still technical challenges under research.

Chapter 3

Electromagnetic Energy Harvester

During this stage, different coils prototypes with a moving magnet inside of them were constructed. The motion of the magnet will be caused by the ambient vibration inside a train, which will encounter a change in magnetic flux density, which produces an electromotive force in the coil. This system was examined to function as an energy harvester to be used inside a carriage of a train.

3.1 Working principle

The physical phenomenon behind this type of harvester is called electromagnetic induction. This happens when a coil suffers displacement regarding a magnetic field, or when the opposite occurs, making an electromotive force to be induced. This creates a current flow which can be used to feed a load. Electromagnetic induction is represented on figure 3.1.

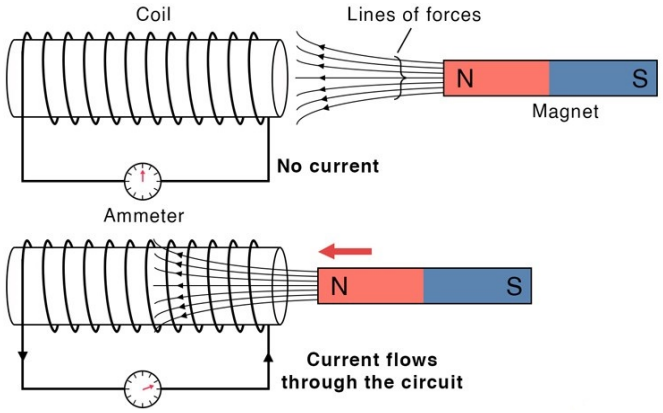

Figure 3.1: Electromagnetic induction. (Retrieved from [30])

During this study, the environmental stimulus considered is vibration which causes the magnet inside the coil to move creating a variation of the magnetic field and, by consequence inducing a current.

3.2 Theoretical analysis

According to the Faraday's Law, the induced voltage known as the electromotive force, ϵ, is proportional to the strength of the magnetic field, B, since it is its variation that induces a voltage. There are also other parameters that influence the electromotive force generated such as the number of coil turns, N, and the cross-section area, A, of the coil, if these values are increased so it is the voltage induced. Equation 3.1 shows how to calculate the voltage induced by the coil, dependent on the magnetic flux density and the characteristics of the coil.

$$V_{coil} = N \cdot \omega \cdot B \cdot A \cdot \mu \tag{3.1}$$

In equation 3.1, μ is the effective magnetic permeability of the core material and ω is the angular frequency.

The magnetic field, B, is produced by the electric current generated, it is a consequence of the moving electric charges. The magnetic field can be calculated according to equation 3.2.

$$B = \mu \cdot \frac{N \cdot i}{\sqrt{4r^2 + l^2}} \tag{3.2}$$

In equation 3.2, r is the radius of the coil and l is its length, finally, i is the induced current. But if $l >> r$ an approximation can be made and the magnetic field can be calculated as presented in equation 3.3.

$$B = \mu \cdot \frac{N \cdot i}{l} \tag{3.3}$$

The magnetic flux, Φ, derives from the magnetic field. It corresponds to the magnetic field over a determined surface, S, as equation 3.4 shows.

$$\Phi_B = \iint_S B \cdot dS \tag{3.4}$$

Based on equation 3.2 and also knowing that these calculations are going to be used for a solenoid shaped coil, whose surface is a circle, the formula that describes the magnetic flux can be written as presented in equation 3.5.

$$\Phi_B = N \cdot B \cdot A = \mu \cdot \frac{N^2 \cdot \pi \cdot r^2}{l} \cdot i \tag{3.5}$$

Finally, the inductance of the coil to be implemented can be calculated following equation 3.6.

$$L = \frac{\Phi_B}{i} = \frac{N \cdot B \cdot A}{i} \tag{3.6}$$

However, by already knowing equation 3.5, it is possible to get a simplification of equation 3.6 to calculate the coil's inductance. This formula is presented in equation 3.7.

$$L = \frac{N^2 \cdot A \cdot \mu}{l} \tag{3.7}$$

In order to calculate the theoretical current generated by the coils that will be studied, equation 3.3 is going to be used due to the fact that all variables are known, except variable B, the magnetic field strength. An approximation is going to be made to obtain an hypothetical peak value of B, because in this application the magnetic field will be varying with time as a consequence of the magnet movement caused by the train.

Therefore, according to a study about the magnetic field related to overhead power lines in which a comparison of different harvesters geometries were considered and compared. [31] The solenoid shaped harvester was simulated with a core conductivity equal to 0 so that the focus was only to observe the magnetic properties. A maximum value of 110 μT_{rms} was obtained based on electromagnetic simulations. This value is going to be used as a reference for the magnetic field strength in further calculations along this chapter.

3.3 Experimental results

Three prototypes of electromagnetic harvesters, coils with a moving magnet, were built. The materials needed were copper wire, a tube, super-glue, tape and a spherical neodymium or cylindrical magnet that fitted inside the tube. Different measures were performed to find the voltage and current generated. The experimental results were compared to the values obtained through theoretical calculations.

3.3.1 First prototype

The first prototype built is presented in figure 3.2. The coil length is 20 cm, its outer diameter is approximately 2 cm and it has 20 windings of copper wire of diameter equal to 1 mm.

The magnet chosen was a neodymium magnet because when compared to ferrite, alnico, and even samarium-cobalt magnets, neodymium magnets are the strongest commercially available. They also offer unmatched levels of magnetism and resistance to demagnetization at a reasonable price. In this experiment, four magnets were used. They are cylindrical, nickel plated, made from neodymium, iron and boron with a 0.5 cm diameter [32].

Since this prototype did not have many windings, the voltage peaks that were produced while the magnet was moving inside the coil could not be distinguished from the noise. Therefore, this prototype had to be upgraded.

Figure 3.2: First electromagnetic harvester prototype implemented.

3.3.2 Second prototype

The second prototype built is the one presented in figure 3.3. This coil has 170 windings of the same cooper wire used on the first prototype, it is 20 cm long and its diameter is 2 cm. An upgrade made on this prototype was the magnet, a spherical neodymium magnet was used for greater ease when moving due to any kind of vibration caused by the train.

Figure 3.3: Second electromagnetic harvester prototype implemented.

The voltage produced by the coil in open circuit while the magnet was moving is 100 mV to 180 mV. The movement was triggered manually and consequently its frequency is very low, around 2 Hz to 5 Hz. The waveform of the voltage generated can be seen in figure 3.4. The red line on figure 3.4 marks the moment when the harvester stopped being stimulated. The majority of the peaks above 50 mV correspond to the movement of the permanent magnet when it went end to end inside the coil.

To calculate the current generated by the coil a resistor of known value

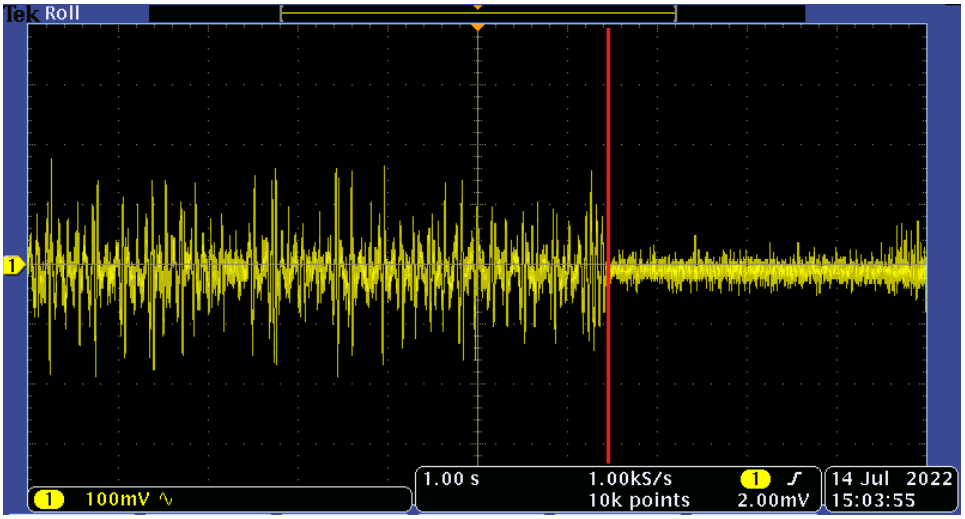

Figure 3.4: Waveform of the voltage produced by the coil in open circuit taken with oscilloscope DPO3052.

---

was used, for this purpose the resistor chosen was 1 Ω. Figure 3.5 shows the voltage drop obtained across the resistor terminals when the magnet was moving with the 1 Ω load. The voltage value is in the range of 30 mV to 125 mV which means that the current generated is also in the range of 30 mA to 125 mA as the load is 1 Ω. Once more, the coil was set in motion manually.

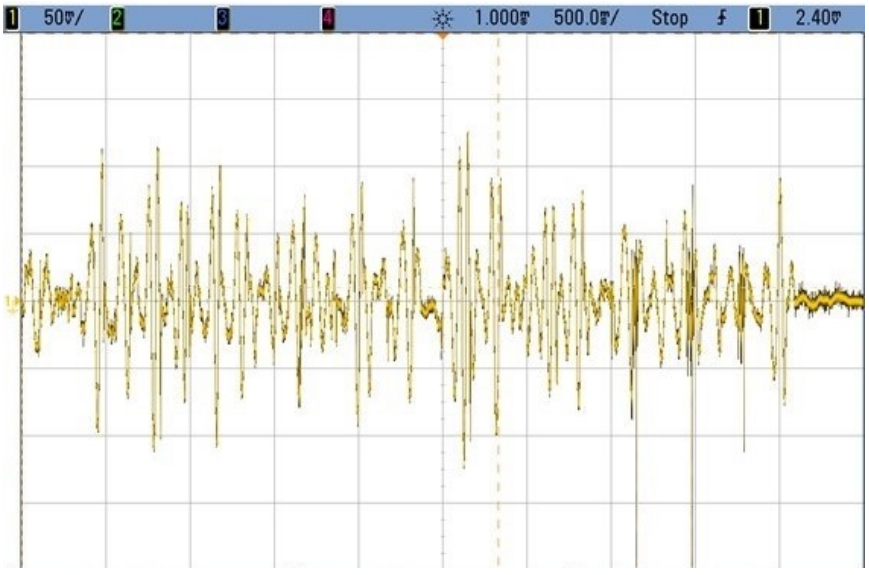

Figure 3.5: Waveform of the voltage produced by the coil with a load of 1 Ω.

3.3.2.1 Use case: Running

A use case was taken into account to better understand whether the voltage generated is raised with increasing frequency. The coil was attached to a person who was moving, which caused the magnet within the coil to move and therefore created a current. For this experiment, it was necessary to use a SparkFun Thing Plus - ESP32 [33] to collect and store the voltage generated and an accommodation circuit to amplify the value to be read by the Analog to Digital Converter (ADC) with an higher resolution.

The microcontroller was programmed on Arduino IDE and the data was collected taking into consideration the frequency of the signal generated by the coil which in a running scenario will have a value from 4 Hz to 8 Hz. So according to Nyquist–Shannon sampling theorem described on equation 3.8, the minimum sampling frequency of an analogical signal for it to be read and converted into a digital one should be more than 16 Hz, so the sampling frequency used was 20 Hz which is bigger than the double of the maximum frequency of the coil's produced signal.

$$f_s > 2.B_w \tag{3.8}$$

In equation 3.8, f_s is the sampling frequency and B is the highest frequency of the signal to be sampled.

For the accommodation circuit, different approaches were considered and implemented. For example, an transimpedance amplifier that would convert the current at the input into voltage at its output, but this did not work due to the low voltage at the input of the amplifier. The final accommodation circuit that allowed to measure the current was the one presented on figure 3.6. It consists of a buffer in order to avoid current loss, since it has a very high input impedance, and then an amplifier with gain equal to 11 so that the value could be read by the ADC.

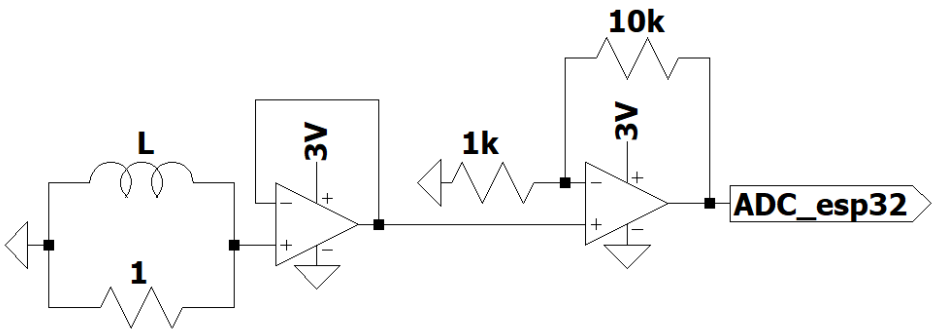

Figure 3.6: Final circuit implemented to measure the current generated by the coil.

When everything described above was working as expected, the exper-

iment got to the next stage, actually running with the coil and magnet. Figure 3.7 shows the voltage produced by the harvester when attached to someone, it only shows positive values because the ADC is only capable of reading positive voltages. It should be noticed once more that both, voltage and current, have the same value because the load is 1 Ω. During this experiment, the maximum current and voltage produced were around 100 mA/mV and the maximum power the harvester produced was around 9 mW.

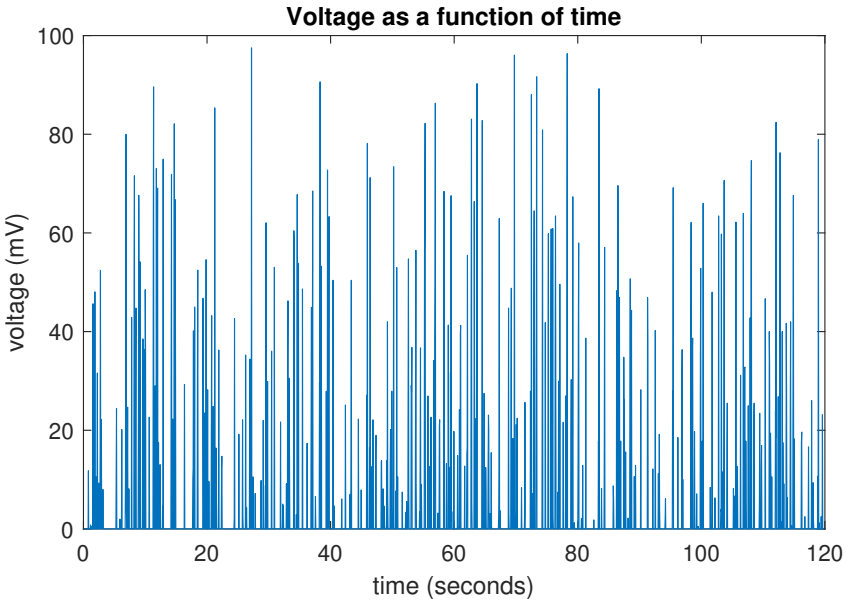

Figure 3.7: Waveform of the voltage/current produced by the coil, when attached to someone running, with a load of 1 Ω.

3.3.2.2 Validation of the experimental current

As explained in section 3.2, the theoretical calculation of the current generated will be done according to equation 3.3 using the magnetic field value obtained in literature [31]. Therefore, according to the assumptions made, the current generated by this harvester would have a maximum value of 138 mA. This value is in the same order of magnitude as the value obtained experimentally and it is also according to the results achieved with the running test performed, although the magnetic field value used is an approximation for slightly different conditions.

3.3.3 Third prototype

Despite the fact that the current generated by the second prototype is significant, it doesn't produce enough voltage for it to function properly as an energy harvester. Regarding the poor results achieved, more improvements had to be thought about. For example, using thinner copper wire since it allows the coil to have more windings which has direct relation with the induced voltage according to equation 3.1. Also, the cross-section area was reduced comparing to the previous coils, in order to use the minimum length of copper wire possible, so it does not increase the coil's resistance.

Thereby, a new coil was manually built and the result can be seen on figure 3.8. It is 20 cm long, its outer diameter is around 1.5 cm, less than before, and has approximately 330 windings made of 0.05 mm width copper wire.

Figure 3.8: Third electromagnetic harvester prototype built.

Given the upgrades made on this new coil, an increased value of the generated power was expected. This was confirmed based on the measurements made in open circuit as it is possible to see in figure 3.9. By looking at figure 3.9 it is clear that the third prototype produces a bigger voltage than the second prototype in the same conditions and measured in open circuit. The peak average voltage generated by this coil it is around 200 mV as is possible to see in figure 3.9.

To calculate the current generated by this upgraded prototype, the coil was then tested with a 1 Ω and new measurements were made. The result can be seen in figure 3.10 which shows a print screen of the signal on the oscilloscope when the coil was manually moved. By looking at figure 3.10 and knowing that the load resistor is equal to 1 Ω, once again the voltage

Figure 3.9: Waveform of the voltage produced by the third coil in open circuit taken with oscilloscope DSOS804.

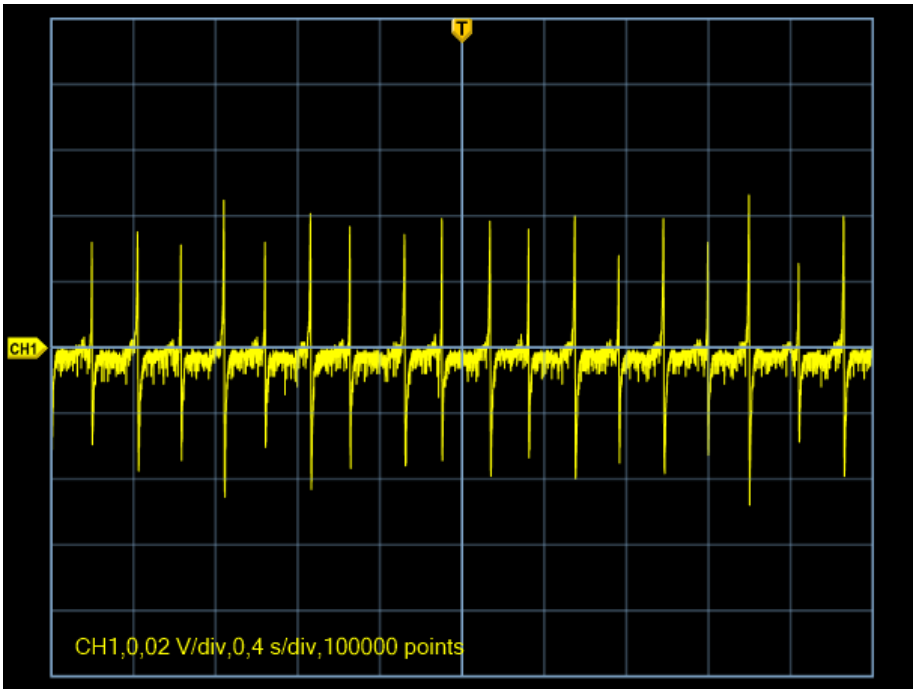

Figure 3.10: Waveform of the voltage produced by the third coil with a load of 1 Ω taken with oscilloscope DPO3052.

and the current will have the same value. With that said, the maximum voltage and current generated by the third prototype is approximately 45 mV/mA. This outcome doesn't meet the previous expectations.

Despite the upgrades done, the power generated by the third coil is lower than the generated by the second coil. There are a number of factors that could explain why this drop occurred, but the most obvious ones are related to the modifications made to the third prototype in comparison to the second. The first change was the reduction of the cross-section area obtained by using a thinner coil which was a bad choice since it increases the coil resistance and decreases the voltage generated according to 3.1. The second change was the width of the cooper wire used, it was chosen a thinner wire in order to allow more turns, that would increase the voltage produced. But, because, there were more turns, which required using a longer piece of copper wire, the parasitic resistance of the coil also increased. So, not only the coil's parasitic resistance suffered an increment related to the smaller cross-section area, but also more wire was used making the resistance greatly increase too. These two facts combined may explain the results obtained.

3.3.4 Rectification

The coil generates an AC signal as it can be seen in previous sections, this is not useful being an harvester whose goal is to power a device. Thus, the next step was to rectify the AC signal to turn it into a DC one for it to be able to be stored and used to power a device.

The low voltage produced by the harvester is an issue since the output of the rectification is equal to the input voltage (output of the harvester) minus the forward voltage drop of the diodes. This implies that the rectified output will have an even lower value, resulting in a residual and unusable voltage. To solve the stated problem, the type and behaviour of the diode chosen is crucial and its characteristics have to be highly considered.

A Schottky diode is the best option since there are many of them available on the market with a very low forward voltage drop. And also because of one of the main characteristics of this kind of diodes, the fact that they start conducting before the knee voltage is reached when comparing to a p-n junction diode as can be seen in figure 3.11. This means that the diode will start to conduct at a lower voltage than its forward voltage, although with very low current. Given this, a Schottky diode with a low breakdown voltage had to be chosen for it to be suitable in this kind of application. The SMS7630-061 diode [34] is characterised by a voltage forward drop around 60 mV .

All rectifier circuits were designed on LTSpice in order to understand their viability. The first circuit tested was a full-wave rectifier bridge with a super capacitor, since the harvester is low frequency. The schematic of a full-wave bridge rectifier can be seen in figure 3.12.

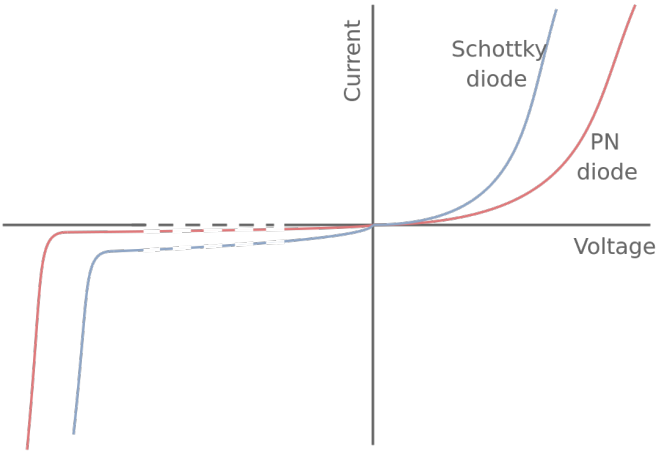

Figure 3.11: Voltage-current characteristic of a p-n junction diode and Schottky diode. (Retrieved from [35])

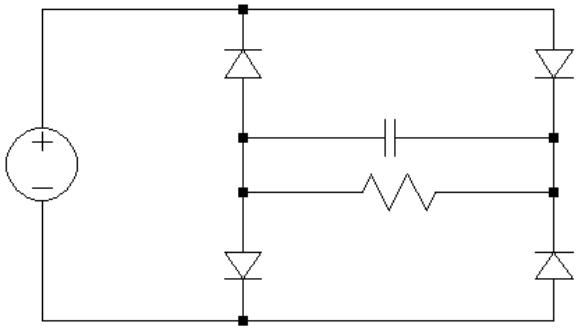

Figure 3.12: Schematic of a brigde rectifier.

The harvester was simulated as a voltage source using real data retrieved from a test previously performed and also using the SMS7630-061 model for the diodes. Since this harvester would work at a maximum frequency around 5 Hz in a scenario which would be implemented on a train, the resistor and capacitor have to be chosen accordingly so that the capacitor has enough time to be charged through the resistor. The best values for the resistor and capacitor can be determined according to formula 3.9.

$$f_c = \frac{1}{2\pi RC} \tag{3.9}$$

After designing and implementing the bridge rectifier, the results obtained were not good. Figure 3.13 shows the results that contribute to the conclusion that even with a rectifier made of Schottky diodes with such low forward voltage drop, with this rectifier circuit, the rectification is not

achieved due to the low voltage at the input, generated by the harvester. Other Schottky diodes could have been considered for this application since there are more available on the market, but below 60 mV there aren't so many, and the ones that are available are quite costly and stock-limited.

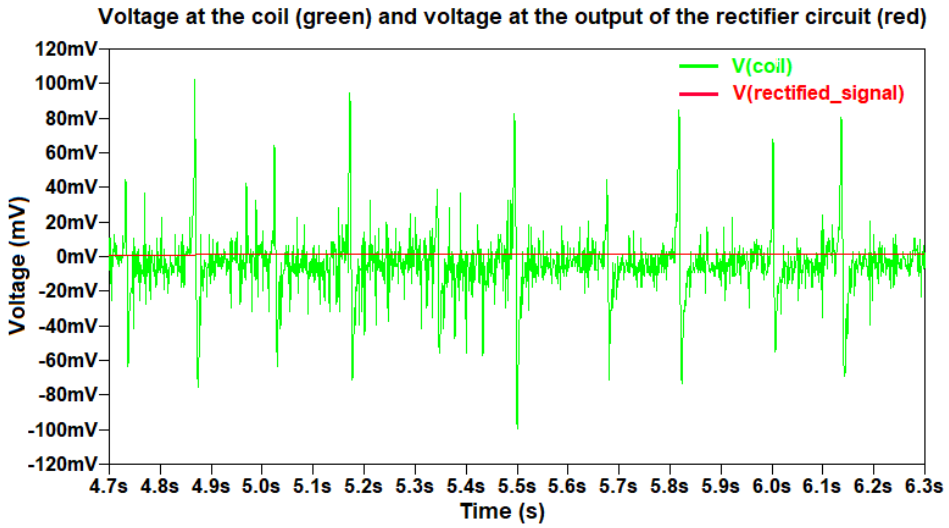

Figure 3.13: Input (green) and output (red) of the bridge rectifier circuit.

Therefore, another type of rectifier circuit was considered, the voltage doubler rectifier. The advantage of this circuit comparing to the bridge rectifier is the fact that the DC output voltage will be doubled probably leading to a voltage that is significant to power a device. This occurs due to the first capacitor and diode following the source that ideally stop the signal from dropping below 0V, this is called a clamp circuit. Consequently, the output of this rectifier topology will be the double of the input less the forward voltage of the Schottky diode. Yet, there is unavoidably a drawback, this approach also doubles the ripple of the output. Figure 3.14 shows the schematic of a doubler rectifier.

The results obtained with the double rectifier are better, as expected, which can be seen in figure 3.15. The output signal goes from 18 to 27 mV, so the ripple has a value of approximately 11 mV.

Although the results with the doubler rectifier are better, they are still not ideal for this prototype to work as an harvester. More upgrades have to be done to this prototype, but it is clear that this doubler rectifier is the best option to use with the type of harvester considered since the value of the voltage produced will always be a problem due to its small amount.

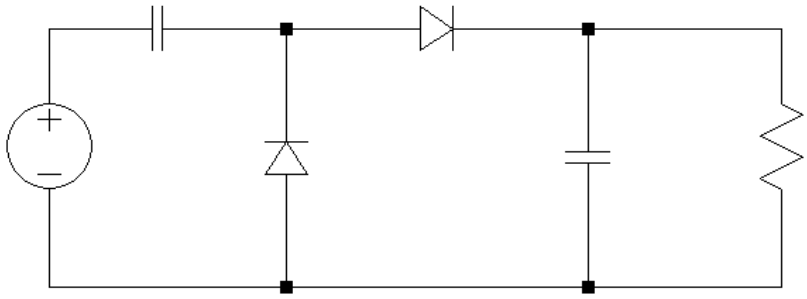

Figure 3.14: Schematic of a doubler rectifier.

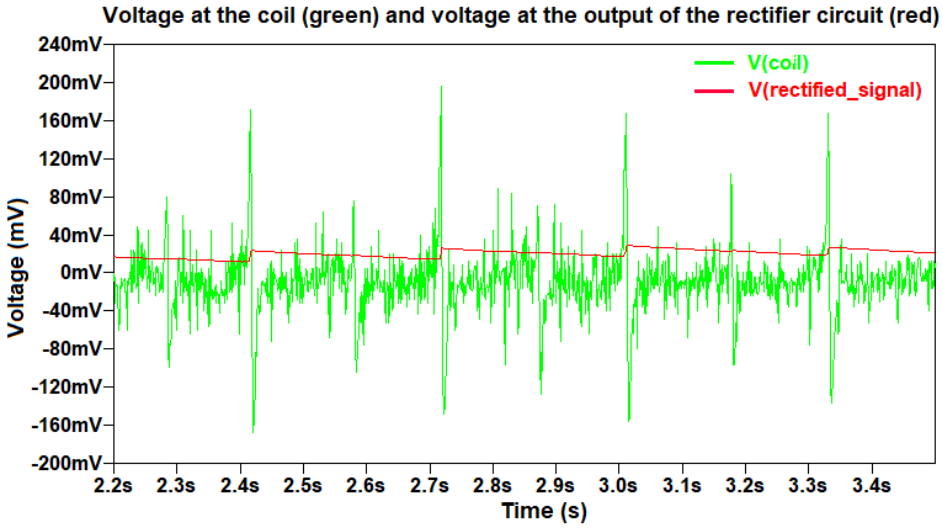

Figure 3.15: Input (green) and output (red) of the doubler rectifier circuit.

3.3.5 Summary

Along chapter 2, different prototypes were built, tested and evaluated to determine whether they have the potential to function as an energy harvester or not.

The results obtained were not satisfactory due to the major limitation of this kind of harvester: the low voltage produced. However, it is shown that with some upgrades such as more turns of wire, so the thinner the copper wire the better, it might increase the voltage produced and consequently the power generated as it was possible to verify with the second prototype. However, the cross-section area of the coil should not be decreased since it increases the parasitic resistance of the coil and, as a consequence, makes its power to be dissipated as it was possible to observe through the third prototype.

Additionally, since rectification is essential for converting the power generated by the harvester into usable energy for a device, different approaches to rectify the signal were studied and simulated. The choice of the right diode to use is also crucial. Taking in consideration the low input voltage, the best approach was achieved for a double rectifier with the SMS7630-061 Schottky diode.

Despite the fact that after rectification the third prototype in open circuit produced an average voltage of 23 mV, this result is not satisfactory with regard to the goal of powering a sensor. Although the prototype developed would not be useful as an harvester, it could be used as a sensor for motion detection applications in which the sensor would have to be attached to the moving object.

Chapter 4

Piezoelectric Energy Harvester

The kinetic energy harvester analysed in this chapter is a piezoelectric. Various piezoelectric materials, namely Lead zirconate titanate (PZT) and Potassium-sodium niobate (KNN), were analysed at this stage. Despite the fact that PZT piezoelectrics contain lead, it is important to note that they are compliant to the Restriction of Hazardous Substances Directive (Rohs). However, given the environmental problems brought on by lead's use in electronics, it is vital to look at alternative materials as KNN.

The goal is to see how power production is influenced by frequency. This will help to better choose the right piezoelectric based on each application, in this case the purpose is to use the harvester in a railway IoT scenario, inside of a train's carriage.

4.1 Working principle

The piezoelectric effect occurs either directly, when the transducer suffers deformation which is converted to electricity, or inversely, when a voltage is applied to the transducer causing deformation. During this chapter, the direct piezoelectric effect is the only one considered.

This effect occurs by applying mechanical energy to a piezoelectric crystal. At first, the material is balanced and there is no electric current but when mechanical pressure is applied to the material through the metal plates, it forces the electric charges within the crystal out of balance. On opposing sides of the crystal face, excess positive and negative charges can be observed. The metal plate then gathers these charges and a voltage and current is created. This is represented in figure 4.1.

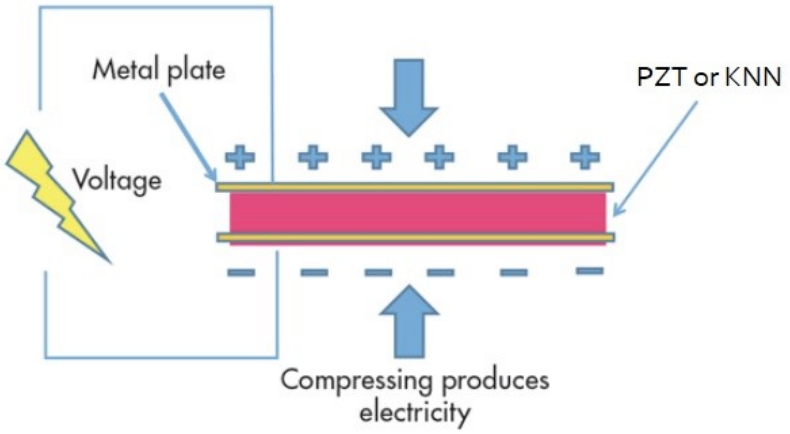

Figure 4.1: Direct piezoelectric effect. (Retrieved from [36])

This effect can be described according to equation 4.1 that refers to the relationship between electrical and mechanical strain.

$$D = d.T + \epsilon.E \tag{4.1}$$

D denotes the electric displacement vector, d is the piezoelectric coefficient, which refers to the quantity of electric current produced by each Newton of force exerted on the material, T represents the mechanical tension per square meter, ϵ is the material dielectric permittivity and E represents the electric field.

4.2 Piezoelectric's characteristics

Piezoelectrics materials can be natural, such as quartz, or synthetic, like PZT or KNN. On a general manner, synthetic materials are considered to be more efficient meaning that they can produce more voltage for the same amount of applied mechanical stress when comparing to natural materials, as they have a bigger piezoelectric charge coefficient, d_ij. This coefficient is defined according to two variables that describe the polarization of the material. The polarization can occur according to two different modes for piezoelectric materials, 31 or 33, but normally they are used according to 33, which means that both the deformation suffered by the crystal and the electric field are in the same direction whereas mode 31 have them in opposite direction and consequently the coupling factor is smaller than in mode 33.

When choosing a piezoelectric more parameters are important to consider as the electromechanical coupling factor of a piezoelectric that measures the percentage of mechanical energy that may be transformed into

electrical energy and vice versa; the dielectric constant, since it has a big influence on the conductivity of the transducer, in practice it should be as significant as possible in an environment characterised by vibration of very low acceleration; the dielectric loss factor (loss tangent), that should be as small as possible; finally, the Curie temperature, it determines that above a certain temperature the piezoelectric material loses their piezoelectricity, so it it can be a limitation for high temperature applications.

Resonant frequency is another parameter to pay attention since this is the frequency at which the conversion of mechanical into electrical energy is more efficient. However, these transducers are usually used below that frequency so that the phase shift between the input signal and output signal is decreased. The resonant frequency depends on different factors such as the volume, shape and material of the transducer itself. For instance, the thicker the piezoelectric the lower is the resonant frequency.

For this study, PZT, as shown in figure 4.2a, and KNN piezoelectrics, as shown in figure 4.2b, were selected to be tested. The transducers chosen are listed and described on table 4.1. It's important to note that the resonant frequency is a value given by the manufacturer which is measured when the piezoelectric is in open circuit and one of its extremities is fixed to a mass that is much bigger comparing to the transducer.

#	*Model*	*Resonant freq.*(Hz)	*Diameter*(mm)	*Material*
1	CEB-20D64	$6.5k$	20	PZT
2	Aveiro Univ.	*unknown*	50	KNN
3	Aveiro Univ.	*unknown*	50	KNN
4	7BB-12-9	$9k$	12	PZT
5	7BB-41-2	$2.2k$	41	PZT
6	7BB-20-3	$3.6k$	20	PZT

Table 4.1: Piezoelectric samples: models and characteristics.

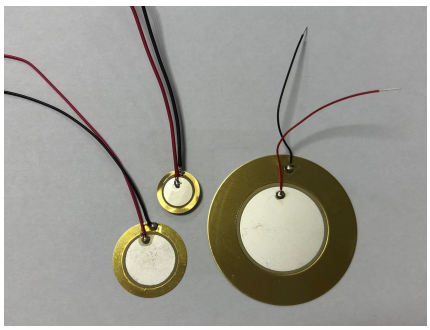

(a) PZT piezoelectric.

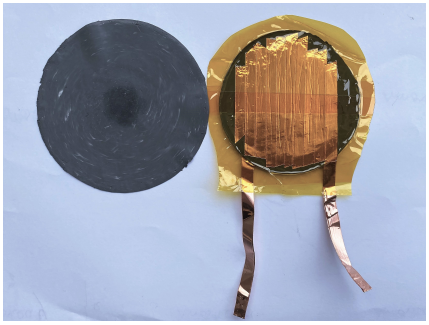

(b) KNN piezoelectric.

Figure 4.2: Piezoelectrics analysed: PZT and KNN.

Sample number 1 is a model of CUI Devices [37] and sample number 3 to 6 are Murata's models [38], those are shown in figure 4.2a. Sample 2 and 3, made of KNN, were given by the Materials and Ceramic Department of Aveiro University, since it was object of study of a master thesis there. One of these piezoelectrics can be seen in figure 4.2b.

4.3 Piezoelectrics along frequency

In order to study the behaviour of different piezoelectric transducers (in open circuit) with frequency and better choose the right transducer to each application, a study along frequency was performed.

With that goal in mind the idea was to create conditions as real as possible to test the piezoelectrics, inside a laboratory, simulating the vibration that a piezoelectric would be normally exposed through sound or mechanical waves. Given this, a signal generator was used to do a frequency sweep from 1 Hz to 10k Hz. And also, a mini-shaker[39] which was the key tool to perform this test because it made possible to apply the signal to the piezoelectric like it would happen in real life applications. The data was then collected using an oscilloscope linked to the computer using Virtual Instrument Software Architecture (VISA) and the results were later analysed employing Matlab's tools. The system described above can be seen in form of a diagram in figure 4.3.

Figure 4.3: System diagram of the measurements performed.

A study on interior noise and vibration of metro vehicles carried in Guangzhou, China showed that the interior noise and vibration of the floor and sidewalls were in the range of low to middle frequency. Within this range, there were two frequencies subranges that proved to be independent of the train's speed: 125 to 250 Hz whose center frequency is 160 Hz and 400 to 1k Hz with a center frequency at 800 Hz. [40]

4.3.1 Setup

The experimental setup can be seen in figure 4.4. The input signal was a sinusoidal generated by 33250A Agilent Signal Generator whose frequency was swept from 1 to 10k Hz with an amplitude of 2.85 dBm for all tests performed, this is the equipment on the left side in figure 4.4. On the middle, in figure 4.4, it is possible to see the shaker that receives the signal generated previously and applies it to the piezoelectric. On the right of figure 4.4 it is shown the Tektronix Oscilloscope DPO3052 which allowed to retrieve the

data obtained to be analysed afterwards on Matlab. The piezoelectric is put on the surface of the shaker as shown in figure 4.5.

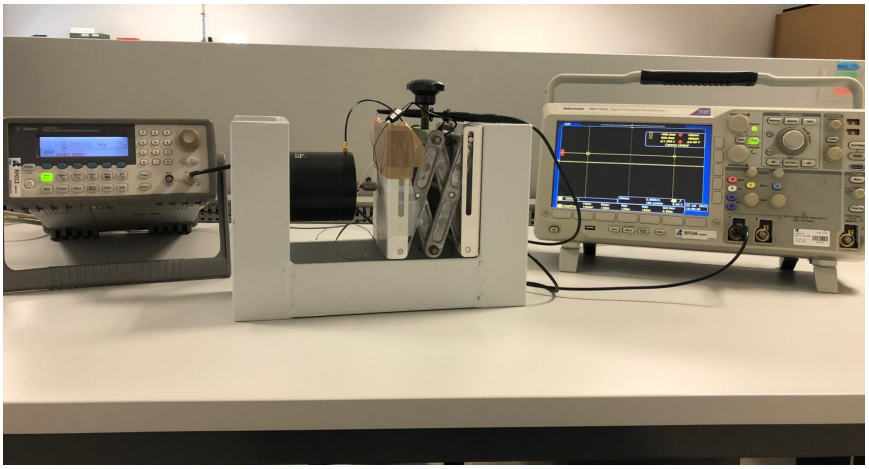

Figure 4.4: Experimental setup to test piezoelectrics.

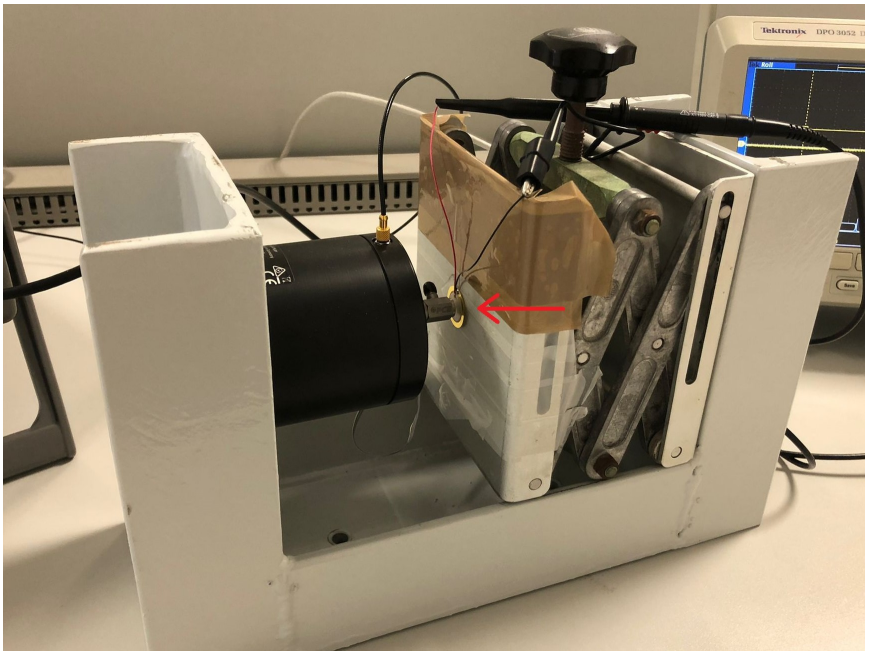

Figure 4.5: Piezoelectric attached to the shaker.

4.3.2 Experimental results

After finishing the retrieving of data of all measurements, the data collected was analysed on Matlab where the maximum peak to peak voltage for each frequency and sample was calculated. Also, the power generated by each sample at every frequency tested was calculated according to 4.2 with the help of the Matlab function *trapz*() that computes the integral's value using the trapezoidal method. This mathematical method divides the area into trapezoids with easier-to-compute areas, which roughly approximates the integration within an interval as shown in figure 4.6.

$$P = \frac{1}{R}\int_0^{\delta t} v(t)^2\, dt \tag{4.2}$$

R is the load resistor which was used to perform the measurements (in this case it was 1 $M\omega$ because of the probe's resistance that was used) , δt is one second for every sample and every frequency so that a comparison between them can be made, $v(t)$ is the voltage data collected from the oscilloscope and t is the internal variable of integration.

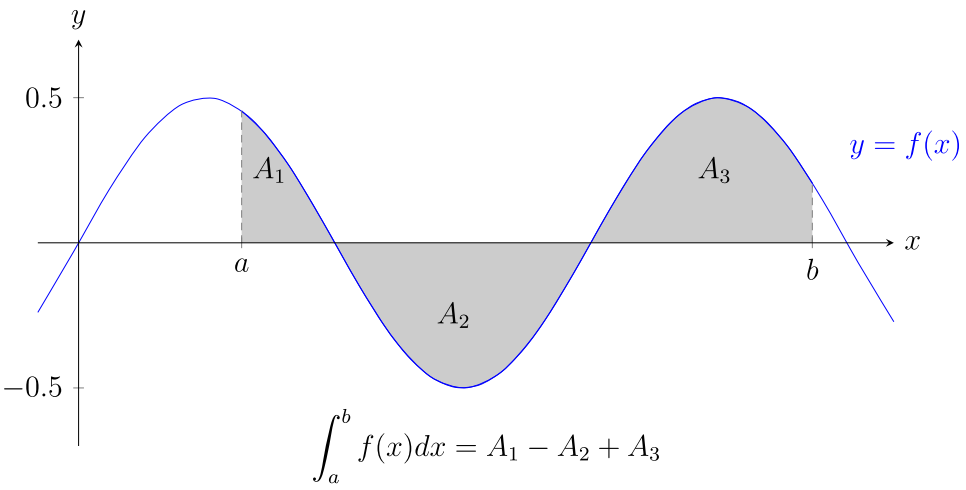

Figure 4.6: Illustration of an integral calculation through trapezoidal method. (Retrieved from [41])

For sample number 1 of the table 4.1, which is a ceramic PZT transducer, the sweep in frequency was carried and for each frequency the waveform was collected as it is shown in figure 4.7a and 4.7b that presents the behaviour of the piezoelectric when a signal of 500 Hz and 5k Hz, respectively, is applied through the mini-shaker .

All waveforms are periodic as it is possible to see in figure 4.7a and 4.7b. After collecting the waveforms associated to all frequencies tested, the results were treated and analysed on Matlab to see how the piezoelectric behavior changes with frequency. This is presented in figure 4.8.

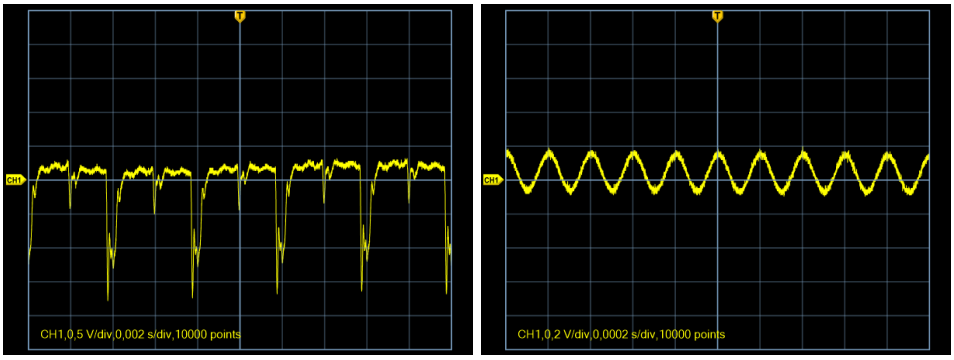

(a) Signal of 500 Hz. (b) Signal of $5k$ Hz.

Figure 4.7: Waveform that piezoelectric number 1 of the table 4.1 generates when a signal is applied, taken with oscilloscope DPO3052.

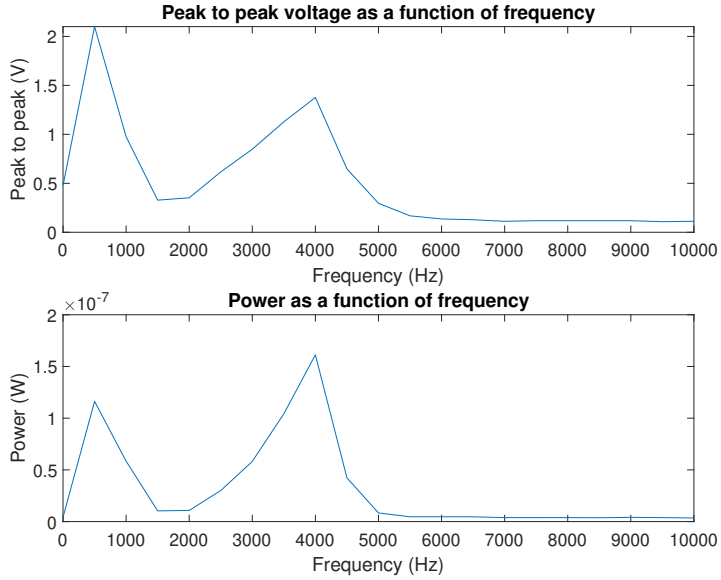

Figure 4.8: Peak to peak voltage and power as a function of frequency of piezoelectric number 1 of the table 4.1.

It can be seen that the voltage amplitude has a direct relation with the power generated, as expected. The maximum peak to peak voltage occurred at 500 Hz with a value of 2.1 V whereas the second maximum value is 1.37 V at 4 kHz. In terms of frequency, this piezoelectric has better performance at low frequencies, namely around 500 Hz and 4 kHz producing a maximum power of 116 nW and 161 nW, respectively.

For sample 2 of the table 4.1, comprised by KNN, the waveforms for 200 and 300 Hz can be seen in figure 4.9, which are graphs that show the behavior across time of the piezoelectric when stimulated. By comparing all waveforms captured, it is observed that for frequencies bigger than 500 Hz the noise is dominant. Once more, these piezoelectrics show a periodic behavior.

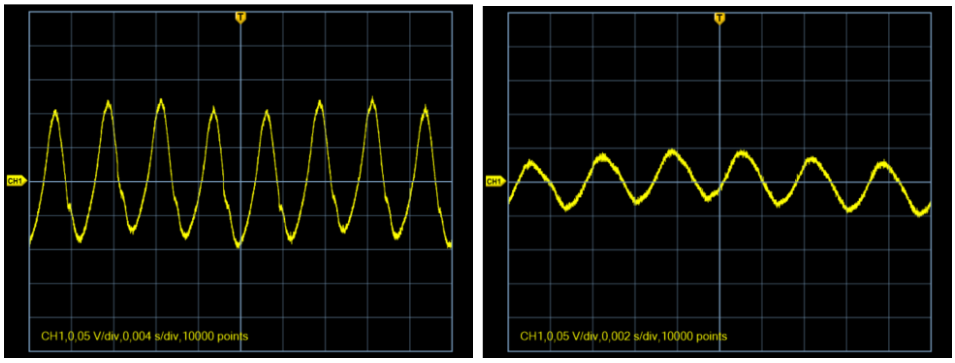

(a) Signal of 200 Hz. (b) Signal of 300 Hz.

Figure 4.9: Waveform that piezoelectric number 2 of the table 4.1 generates when a signal is applied, taken with oscilloscope DPO3052.

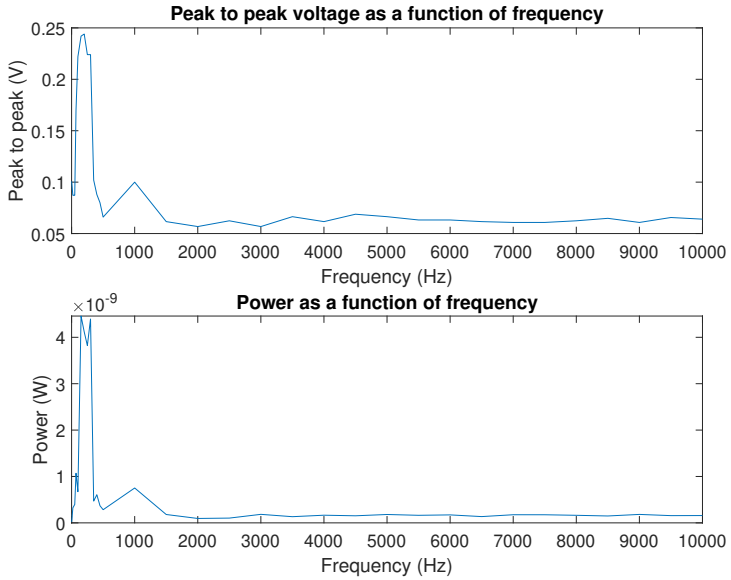

Figure 4.10: Peak to peak voltage and power as a function of frequency of piezoelectric number 2 of the table 4.1.

The final analysis which is presented in figure 4.10 shows that the max-

imum peak to peak voltage is observed for frequencies in the range of 70 to 300 Hz having a maximum value of 244 mV. Regarding the power results, the maximum occurred from 150 to 300 Hz and had a peak of 4.5 nW.

For sample number 3 of the table 4.1, different waveforms are presented in figure 4.11 which shows the output for an input signal of 350 and 500 Hz. From 500 Hz the output signal was mainly dominated by noise.

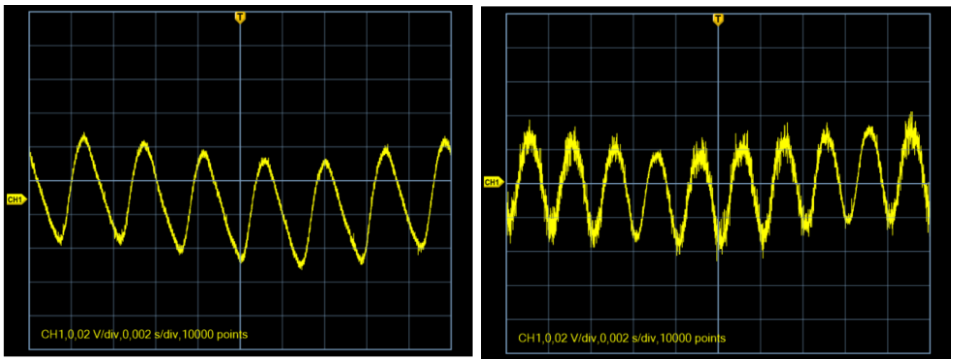

(a) Signal of 350 Hz. (b) Signal of 500 Hz.

Figure 4.11: Waveform that piezoelectric number 3 of the table 4.1 generates when a signal is applied, taken with oscilloscope DPO3052.

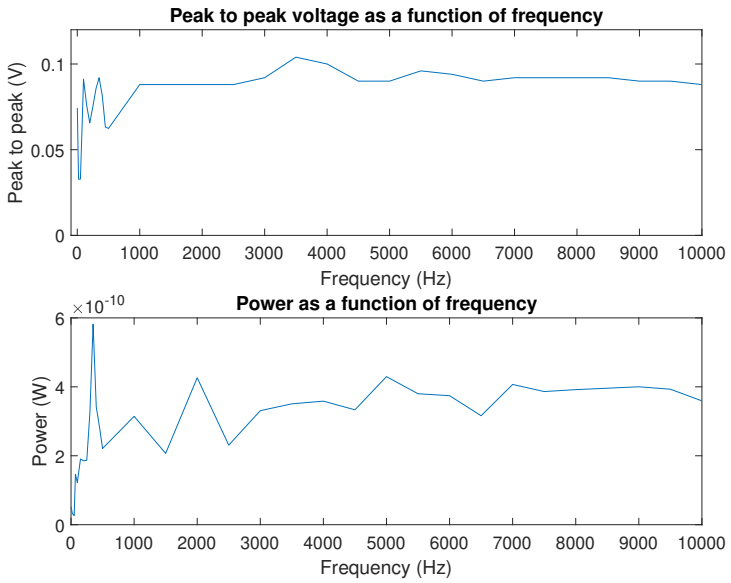

Figure 4.12: Peak to peak voltage and power as a function of frequency of piezoelectric number 3 of the table 4.1.

The results of sample 3 along frequency are shown in figure 4.12. By

observing figure 4.12 it can be seen that the peak to peak voltage is very stable across all frequencies tested above $1k\ Hz$ and has an average value close to 100 mV. When it comes to power, there is a peak around 350 Hz of 581 pW and above $2k\ Hz$ the average power is 374 pW.

Regarding sample number 4 of the table 4.1, its results are displayed in figure 4.13 when the input signal has a frequency of 500 and $4k\ Hz$.

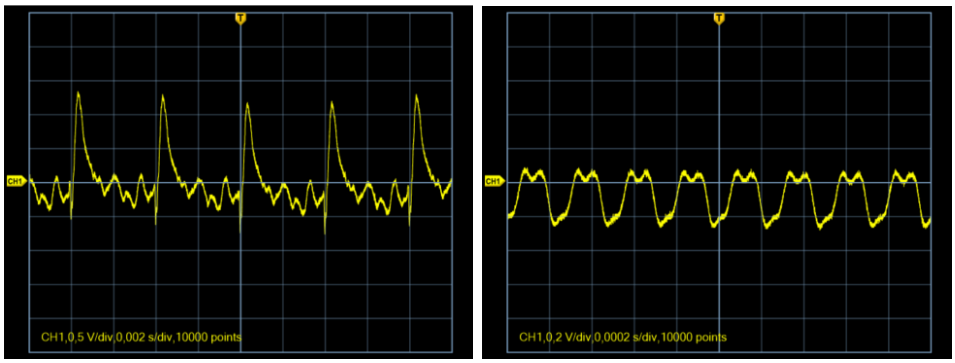

(a) Signal of 500 Hz. (b) Signal of $4k\ Hz$.

Figure 4.13: Waveform that piezoelectric number 4 of the table 4.1 generates when a signal is applied, taken with oscilloscope DPO3052.

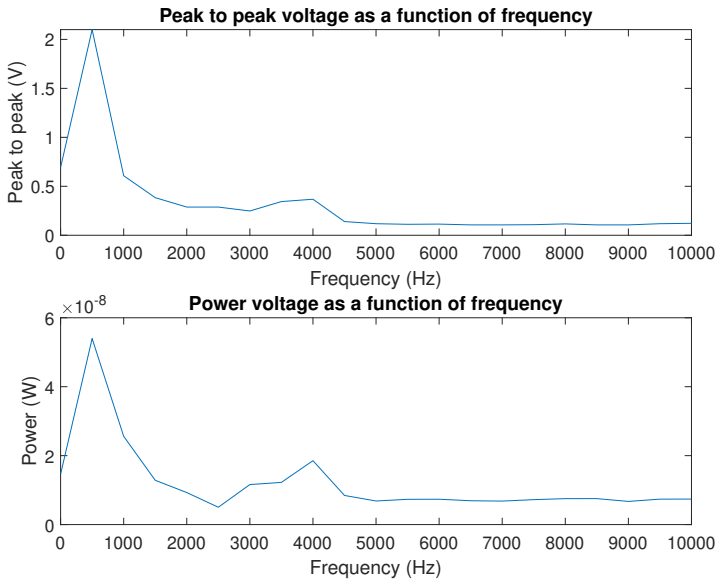

Figure 4.14: Peak to peak voltage and power as a function of frequency of piezoelectric number 4 of the table 4.1.

Figure 4.14 describes the voltage and power generated as a function of

frequency after analysis on Matlab. The maximum peak to peak voltage and power occur for the same frequency, 500 Hz with a 2.1 V and 54 nW, respectively. Above that frequency the power and the voltage amplitude are very low when comparing with the values obtained for 500 Hz.

The waveforms related to sample number 5 of the table 4.1 are depicted for an input signal of frequency 500 and 1.5k Hz in figure 4.15.

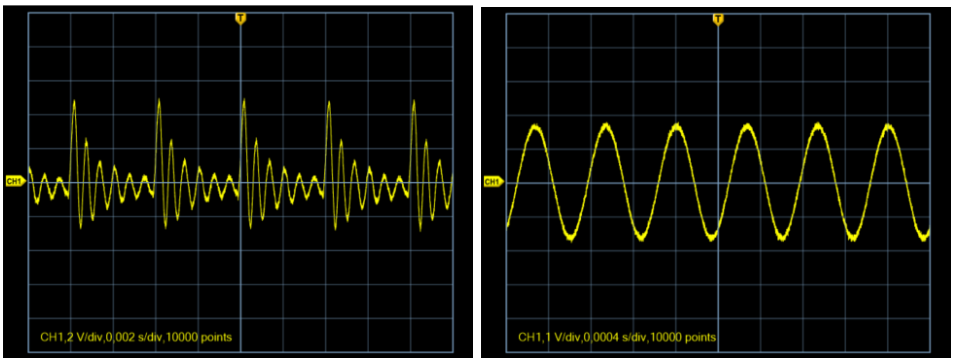

(a) Signal of 500 Hz. (b) Signal of 1.5 kHz.

Figure 4.15: Waveform that piezoelectric number 5 of the table 4.1 generates when a signal is applied, taken with oscilloscope DPO3052.

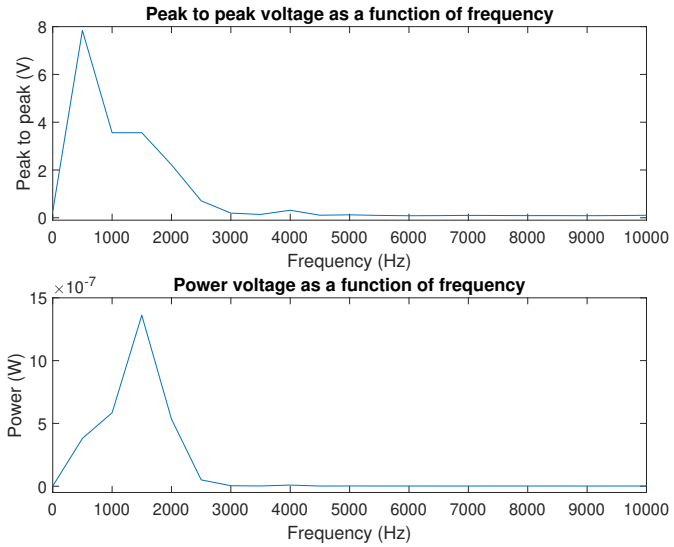

Figure 4.16: Peak to peak voltage and power as a function of frequency of piezoelectric number 5 of the table 4.1.

Figure 4.16 shows the treated results across frequency. By looking at figure 4.16 a maximum value of 7.9 V of peak to peak voltage can be seen

at 500 Hz, this is presented in figure 4.15a. It is also clear that from 3 kHz the voltage is very low, and so is the power. The peak power occurs in the range of 1 to 2 kHz, but its maximum value is 1.36 μW for 1.5 kHz in which the waveform generated can be seen in figure 4.15b.

Finally, for sample 6 of the table 4.1, figure 4.17 show the waveform obtained for a signal of frequency 500 and 4k Hz. The waveforms captured are periodic independently of the frequency that was being tested.

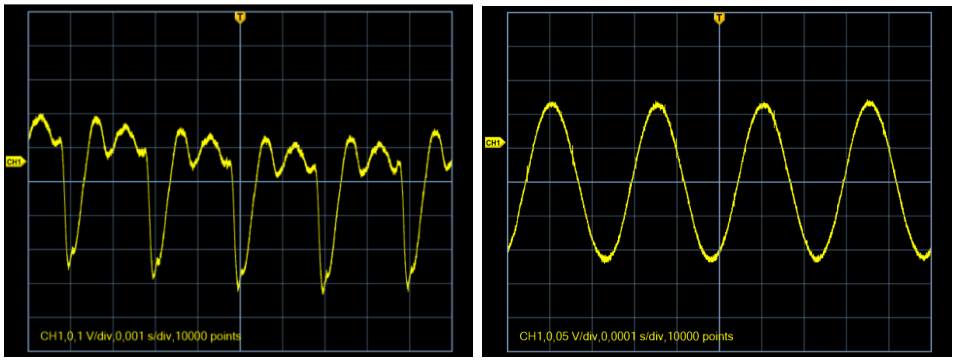

(a) Signal of 500 Hz. (b) Signal of 4 kHz.

Figure 4.17: Waveform that piezoelectric number 6 of the table 4.1 generates when a signal is applied, taken with oscilloscope DPO3052.

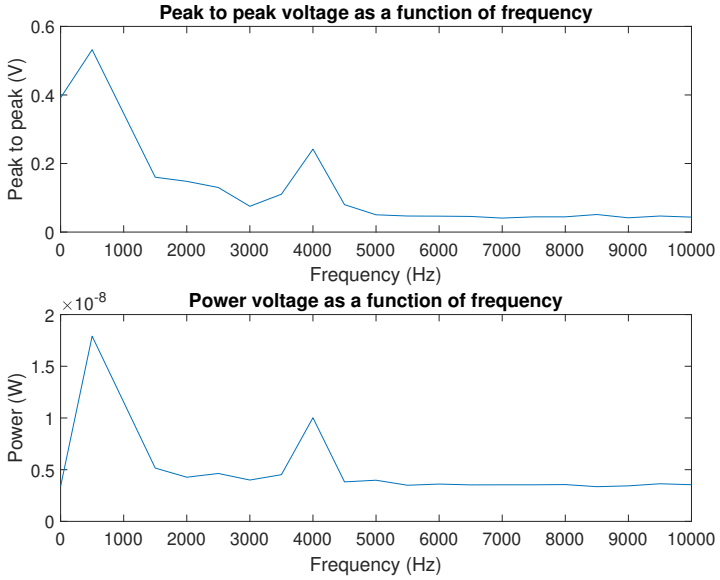

Figure 4.18: Peak to peak voltage and power as a function of frequency of piezoelectric number 6 of the table 4.1.

After treating the data related to the different waveforms it was possible to make an analysis along frequency like shown in figure 4.18. Observing figure 4.18 it is possible to see that the peak to peak voltage is maximum for 500 Hz with a value of 532 mV and there is also a second maximum of 242 mV for 4k Hz. Looking at the power graph, the two maximum values of power are coincident with the maximums of the peak to peak amplitude, having a power of 18 nW for 500 Hz and 10 nW for 4k Hz. The behavior of the piezoelectric is very constant for other frequencies besides 500 Hz and 4k Hz.

4.3.3 Comparisons between piezoelectrics

PZT have been often used in actuators, sensors, transducers and as energy harvesters because of its low-cost and simple production. Additionally, this material is also very popular due to its piezoelectric properties, such as, high dielectric constant, high electromechanical coupling coefficient, high piezoelectric coefficient and high Curie temperature. However, its toxicity is a major issue that has been creating awareness. This material is used so much that lots of variations of the PZT chemical formula are commercially available, two of them and as well as their properties can be found in table 4.2.

As a solution to the stated problem, different options have been studied to substitute PZT, like the one considered in this study: KNN. These lead-free piezoelectrics have showed promising properties, as high Curie temperature, a considerable piezoelectric coefficient and high electromechanical coupling coefficient according to [42].

Table 4.2 shows the main piezoelectric properties of different PZT materials, according to [43] and undoped KNN, according to [42] .

Property	Unit	PZT-5A	PZT-5J	KNN
Piezoelectric Charge Coeff.	pC/N	390	485	80-160
Electromech. Coupling Coeff.	-	0.72	0.74	0.15
Curie temperature	ºC	350	270	420
Dielectric constant	-	1800	2100	393
Dielectric losses	%	0.02	0.02	0.07

Table 4.2: Properties of different piezoelectric materials.

By looking at table 4.2 it is clear that lead based piezoelectric show better characteristics than lead-free transducers. The difference in the piezoelectric charge coefficient is the most significant and the results could easily be explained based on this parameter.

Table 4.3 shows the results and corresponding characteristics of the piezoelectrics considered in this study. By observing table 4.3, is is pos-

sible to conclude that KNN piezoelectric have a much lower produced power when in the same conditions as the PZT. This can be firstly explained due to its lower electromechanical coupling factor that refers to the percentage of the mechanical strain that will be converted to electrical energy, it basically defines its conversion efficiency. But also, the huge difference in the piezoelectric charge coefficient makes the power produced by the same mechanical pressure also lower, when comparing to PZT based piezoelectrics. However, these KNN piezoelectrics show very promising results already, one big advantage that should be noticed is its incredible high Curie temperature that can make piezoelectrics useful to a variety of applications that would not be possible with PZT transducers.

#	Material	Diameter (mm)	$F_{P_{max}}$ (Hz)	$P_{max}(nW)$
1	PZT	20	$4k$	161
2	KNN	50	200	4.5
3	KNN	50	350	0.581
4	PZT	12	500	54
5	PZT	41	$1.5k$	1360
6	PZT	20	500	18

Table 4.3: Piezoelectrics characteristics and results obtained.

Regarding the goal of this study, the understanding of which piezoelectric would be the best fit to use in an IoT railway apllication, the best option appears to be sample number 4, PZT based. The reason that contribute to this choice is the fact that it generates more power at frequencies that are independent of the train's speed, meaning that this signal's frequency will always be present along the way of the train. Therefore, it will allow the transducer to generate more power given that the piezoelectric will be stimulated the whole time the train is in movement.

4.4 Summary

Throughout this chapter a frequency characterization was performed for piezoelectrics that differ in the material they are made of and size. There were six different samples, four of them are PZT piezoelectrics which contain lead. The other two, whose material is still being studied and developed by the Materials and Ceramics Department of Aveiro University, are made of KNN which has proven to be an alternative to PZT piezoelectrics.

The frequency range tested was from 1 to $10k$ Hz and the test utilized a shaker that resembled a train's sidewall or a railway track. The results were evaluated based on the peak to peak voltage amplitude of the generated signal and the power produced by each piezoelectric, both as a function of frequency.

The results obtained show that the PZT piezoelectrics, in open circuit, generate more power at higher frequencies than the KNN transducers in the same conditions. Regarding low frequencies, the KNN transducers still generate less power than the PZT devices. However, the value generated is significant, despite the fact that their piezoelectric properties are very different from PZT properties. Even though research into these KNN piezoelectrics is still ongoing, the results so far are encouraging because while having significantly inferior characteristics than conventional ones, they exhibit behavior over frequency that is quite comparable to PZT results.

Chapter 5

Conclusions and future work

The key conclusions and a summary of the thesis's contents and findings are presented in this chapter. It also includes potential future work and upgrades to the harvesters considered.

5.1 Conclusions

The goal of this work was to find new energy harvesters capable of producing energy to power sensors on a train by using its movement and vibration as a source of energy.

In chapter 1, the background of this work was described, its application as well as social, political and environmental context.

Chapter 2 presents the main concepts related to energy harvesting, what is needed to harvest energy from many different sources and what has already been done regarding those sources.

Chapter 3 refers to an electromagnetic energy harvester that uses movement to generate energy. Various prototypes with different characteristics were built and their voltage and current measured and calculated, but the results were not satisfactory. Even the third prototype which had major upgrades, comparing with the others built, had very unexpected results probably related to the increment of the parasitic resistance of the coil. Still in this matter, rectification is a big challenge because of the low voltage typically produced by this kind of harvesters, but necessary to make the power produced useful. It required a study on different rectifier circuits and on Schottky diodes since the harvester produces a very low voltage. With a doubler rectifier it was possible to achieve an approximate DC voltage of 23 mV, better than the voltage achieved with the bridge rectifier. The study of these harvesters was not successful since they do not produce voltage enough to function as energy harvesters. However, the second and third prototype could work properly as a battery free sensor. For instance, a movement sensor if attached to the moving object, it would be capable of detecting

movement without the need of a battery.

In Chapter 4, a PZT and KNN based piezoelectric vibration harvester were considered and their behavior along frequency studied. Since the resonant frequency of this harvester depends on different factors, railway conditions were simulated in a laboratory and the power produced by the piezoelectrics was calculated in order to better understand what are the best transducers to the application in question. Those transducers were evaluated given the fact that the most common and persistent frequencies present while a train is moving are in the range of 125 to 250 Hz and from 400 to 1000 Hz. Taking these facts in consideration, the most suitable piezoelectric is sample 4, model 7BB-12-9 of Murata manufacturer. This model is capable of generating a power of 54 nW when subjected to a signal of 500 Hz, a frequency value that belongs to the range of interest. If temperature was a constraint, the choice would be sample 2, a KNN piezoelectric that produced a power of 4.5 nW for a signal of 200 Hz. These KNN transducers have shown promising results, it is noteworthy that the power obtained is comparable to the power obtained with PZT piezoelectrics.

5.2 Future work

Regarding the electromagnetic energy harvester, more upgrades can be done such as increasing the number of turns of the copper wire, but not by increasing the coil length's since it is inversely proportional to the electromotive force generated, but, alternatively, by decreasing even more the wire's width. Another upgrade possible is increasing the coil's radius, however this may turn out not suitable for most applications. Also, the choice of an optimal load is important, because a matched load guarantees maximum power transfer. Additionally, in order to maximize the power output, the voltage generated should be increased and the coil's resistance decreased, this can be done by adjusting the core shape (cross-section area) or material. Finally, springs can be placed at the ends of the coil so that the magnet moves with an higher frequency and consequently creates more changes in the magnetic field and induces a current.

The work done on chapter 4 can be continued in order to achieve more efficiency. For example, the resonant frequency can be adjusted according to the frequencies that will appear in a real scenario. The study of the right value of the load to use can be done, it is already known that the higher the load, the lower is the resonant frequency. Another study that could be done is on how to turn a piezoelectric automatically tunable, based on the fact that by varying the position of a mass on a piezoelectric cantilever it can change the resonant frequency. This mass could be moved so that the resonant frequency of the piezoelectric matches the ambient frequencies previously detected.

Bibliography

[1] CP Comboios de Portugal. "*Resultados do 1º trimestre 2022 | CP*". https://www.cp.pt/institucional/pt/comunicacao/notas-imprensa/primeiro-trimestre. Accessed: 14-06-2022.

[2] Statista. "*Internet of Things (IoT) connected devices installed base worldwide from 2015 to 2025(in billions)*". https://www.statista.com/statistics/471264/iot-number-of-connected-devices-worldwide/. Accessed: 14-06-2022.

[3] CNBC. "*The impact of the war in Ukraine on euro area energy markets*". https://www.ecb.europa.eu/pub/economic-bulletin/focus/2022/html/ecb.ebbox202204_01~68ef3c3dc6.en.html. Accessed: 18-05-2022.

[4] "*What is energy harvesting?*" - *ONiO*. https://www.onio.com/article/what-is-energy-harvesting.html. Accessed: 18-05-2022.

[5] Our World in Data. "*Fossil Fuels*". https://ourworldindata.org/fossil-fuels#global-fossil-fuel-consumption. Accessed: 18-05-2022.

[6] D. Zhu, M. J. Tudor, and S. P. Beeby. "*Strategies for increasing the operating frequency range of vibration energy harvesters: a review*". *Measurement Science and Technology*, 21(2):022001, October 2009.

[7] J. P. Thomas, M. A. Qidwai, and J. C. Kellogg. "*Energy scavenging for small-scale unmanned systems*". *Journal of Power Sources*, 159:1494–1509, 9 2006.

[8] Electronic Clinic. "*Photovoltaic Effect or Solar Cell Construction and Working*". https://www.electroniclinic.com/photovoltaic-effect-or-solar-cell-construction-and-working. Accessed: 6-05-2022.

[9] Y. K. Tan and S. K. Panda. "*Energy Harvesting From Hybrid Indoor Ambient Light and Thermal Energy Sources for Enhanced Performance*

of Wireless Sensor Nodes". *IEEE Transactions on Industrial Electronics*, 58(9):4424–4435, 2011.

[10] T. T. Viet and W. Chung. "*High-Efficient Energy Harvester With Flexible Solar Panel for a Wearable Sensor Device*". *IEEE Sensors Journal*, 16(24):9021–9028, 2016.

[11] D. Vizzari, E. Chailleux, S. Lavaud, E. Gennesseaux, and S. Bouron. "*Fraction Factorial Design of a Novel Semi-Transparent Layer for Applications on Solar Roads*". *Infrastructures*, 5(1), 2020.

[12] R. Hesham and A. Soltan. "*Study of Energy Harvesters for Wearable Devices*". pages 259–263. IEEE, October 2020.

[13] A. El-Sayed, K. Tai, M. Biglarbegian, and S. Mahmud. "*A survey on recent energy harvesting mechanisms*". In *2016 IEEE Canadian Conference on Electrical and Computer Engineering (CCECE)*, pages 1–5, 2016.

[14] A. Khaligh, P. Zeng, and C. Zheng. "*Kinetic Energy Harvesting Using Piezoelectric and Electromagnetic Technologies—State of the Art*". *IEEE Transactions on Industrial Electronics*, 57(3):850–860, March 2010.

[15] S. Susilo, S. Abdullah, D. Satria, M. R. Ghifari, and B. A. Hermawan. "*Modeling of electromagnetic energy harvesting from vehicle damper in shock absorber of motorcycle*". *Journal of Physics: Conference Series*, September 2019.

[16] J. Farzidayeri and V. Bedekar. "*Design of a V-Twin with Crank-Slider Mechanism Wind Energy Harvester Using Faradays Law of Electromagnetic Induction for Powering Small Scale Electronic Devices*". *Energies*, 15(17), 2022.

[17] S. Chamanian, S. Baghaee, H. Ulusan, Ö. Zorlu, H.Külah, and E. Uysal-Biyikoglu. "*Powering-up Wireless Sensor Nodes Utilizing Rechargeable Batteries and an Electromagnetic Vibration Energy Harvesting System*". *Energies*, 7:6323–6339, October 2014.

[18] J. Briscoe and S. Dunn. "*Piezoelectric nanogenerators – a review of nanostructured piezoelectric energy harvesters*". *Nano Energy*, 14:15–29, 2015.

[19] E. Nwanji, J. Ugbodaga, and O. Daye. "*Sustainable Means For Energy Generation: A Model For Harnessing Energy From Door Motion Using A Piezo Electric Material.*". 07 2017.

[20] T. Starner. "*Human-powered wearable computing*". *IBM Systems Journal*, 35:618–629, September 1996.

[21] S. P. Beeby, M. J. Tudor, and N. M. White. "*Energy harvesting vibration sources for microsystems applications*". *Measurement Science and Technology*, 17:R175–R195, December 2006.

[22] N. Shinohara. "*Trends in Wireless Power Transfer: WPT Technology for Energy Harvesting, Millimeter-Wave/THz Rectennas, MIMO-WPT, and Advances in Near-Field WPT Applications*". *IEEE Microwave Magazine*, 22:46–59, January 2021.

[23] D. Colaiuda, I. Ulisse, and G. Ferri. "*Rectifiers' Design and Optimization for a Dual-Channel RF Energy Harvester*". *Journal of Low Power Electronics and Applications*, 10(2), 2020.

[24] V. Talla, B. Kellogg, S. Gollakota, and J. R. Smith. "*Battery-Free Cellphone*". *Proceedings of the ACM on Interactive, Mobile, Wearable and Ubiquitous Technologies*, January:1–20, June 2017.

[25] L. Gabrillo, M. Galesand, and J. Horan. "*Enhanced RF to DC converter with LC resonant circuit*". *IOP Conference Series: Materials Science and Engineering*, 79:012011, 06 2015.

[26] J. Tissier, M. Koohestani, and M. Latrach. "*A Comparative Study of Conventional Rectifier Topologies for Low Power RF Energy Harvesting*". pages 569–572. IEEE, June 2019.

[27] X. Lu and S. Yang. "*Thermal energy harvesting for WSNs*". pages 3045–3052. IEEE, October 2010.

[28] A. Mukheriee and T. Saha. "*Precision Thermocouple Amplifier for Substrate Temperature Monitoring in an ECR-PE Nano-Film Deposition System*". In *2018 2nd International Conference on Electronics, Materials Engineering & Nano-Technology (IEMENTech)*, pages 1–5, 2018.

[29] M. Kishi, H. Nemoto, T. Hamao, M. Yamamoto, S. Sudou, M. Mandai, and S. Yamamoto. "*Micro thermoelectric modules and their application to wristwatches as an energy source*". pages 301–307. IEEE, 1999.

[30] ScienceFacts. "*Electromagnetic Induction*". `https://www.sciencefacts.net/electromagnetic-induction.html`. Accessed: 05-04-2022.

[31] S. Yuan, Y. Huang, J. Zhou, Q. Xu, C. Song, and P. Thompson. "*Magnetic Field Energy Harvesting Under Overhead Power Lines*". *IEEE Transactions on Power Electronics*, 30(11):6191–6202, 2015.

[32] Cosmus Group. "*Magnet - Cylindrical - Nickel Plated: Datasheet*". https://comus-intl.com/wp-content/uploads/2013/11/M1219-22.pdf. Accessed: 11-04-2022.

[33] Expressif Systems. "*ESP32-WROOM-32 Datasheet*". https://cdn.sparkfun.com/assets/learn_tutorials/8/5/2/esp32-wroom-32_datasheet_en.pdf. Accessed: 14-04-2022.

[34] Skyworks. "*SMS7630-061: Surface-Mount, 0201 Zero Bias Silicon Schottky Detector Diode* ". https://www.skyworksinc.com/-/media/SkyWorks/Documents/Products/101-200/SMS7630-061_201295J_Discontinued.pdf. Accessed: 25-07-2022.

[35] Electronics Notes. "*Understanding Schottky Diode Characteristics & Specifications*". https://www.electronics-notes.com/articles/electronic_components/diode/schottky-\barrier-diode-characteristics-specifications-parameters.php. Accessed: 22-06-2022.

[36] Electronic Design. "*What is the Piezoelectric Effect?*". https://www.electronicdesign.com/power-management/article/21801833/what-is-the-piezoelectric-effect. Accessed: 2-09-2022.

[37] CUI Devices. "*CEB-20D64: 20 mm Piezo Buzzer Element w/Lead Wires*". https://www.cuidevices.com/product/resource/ceb-20d64.pdf. Accessed: 4-07-2022.

[38] Murata Manufacturing Co. "*Piezoelectric Sound Components P37E.pdf EU RoHS Compliant*". https://www.murata.com/en-eu/support/, 2021. Accessed: 5-07-2022.

[39] Brüel & Kjær. "*Mini-shaker Type 4810 – Brüel & Kjær Sound & Vibration*". https://www.bksv.com/pt/instruments/vibration-testing-equipment/measurement-exciters/mini-shaker-type-4810. Accessed: 26-07-2022.

[40] L. Yan, Z. Chen, Y. Zou, X. He, C. Cai, K. Yu, and X. Zhu. "*Field Study of the Interior Noise and Vibration of a Metro Vehicle Running on a Viaduct: A Case Study in Guangzhou*". *International Journal of Environmental Research and Public Health*, 17:2807, 04 2020.

[41] SFU. "*Calculus Early Transcendentals: Integral & Multi-Variable Calculus for Social Sciences*". https://www.sfu.ca/math-coursenotes/Math%20158%20Course%20Notes/sec_defint.html. Accessed: 9-06-2022.

[42] M. Dolhen, A. Mahajan, R. Pinho, M. E. Costa, G. Trolliard, and P. M. Vilarinho. "*Sodium potassium niobate (K0.5Na0.5NbO3, KNN) thick films by electrophoretic deposition*". *RSC Advances*, 5:4698–4706, 2015.

[43] Piezo.com. "*Materials Technical Data (Typical Values)*". `https://info.piezo.com/hubfs/Data-Sheets/piezo-material-properties-data-sheet-20201112.pdf`. Accessed: 7-09-2022.